Pathology International 2003; **53**: 214–220

Original Article

Responsiveness of chemotherapy based on the histological type and Wilms' tumor suppressor gene mutation in bilateral Wilms' tumor

Rie Shibata,[1] Ayako Takata,[1] Akinori Hashiguchi,[1] Akihiro Umezawa,[1] Taketo Yamada[1] and Jun-ichi Hata[1,2]

[1]*Department of Pathology, Keio University School of Medicine, and* [2]*National Research Institute for Child Health and Development, Tokyo, Japan*

To clarify a characteristic of bilateral Wilms' tumor (WT), we examined the clinical and histological features, chemotherapy response and mutations in Wilms' tumor suppressor gene (*WT1*) in five patients. Deoxyribonucleic acid was extracted from peripheral lymphocytes and tumor samples, and direct DNA sequencing was performed to detect *WT1* mutations. Paraffin sections were stained with H&E for histological review and immunostained with anti-*WT1*, anti-Ki-67, anti-S-100 protein and antimyogenin antibodies. In contrast to the single case of epithelial-type WT, the other four cases were fetal rhabdomyomatous nephroblastoma (FRN) or contained a premature skeletal muscle component and appeared to be resistant to chemotherapy because there was no reduction in tumor volume. However, after chemotherapy, most of the tumor components changed into mature striated muscle cells, most of which immunostained almost completely negative for Ki-67. All four cases had the same point mutation of *WT1*. From our results, the histological findings correlated with *WT1* mutations in bilateral WT. The tumor volume of FRN did not decrease in response to chemotherapy. It is possible to predict the chemotherapy response by examining bilateral WT for *WT1* mutations and the histological characteristics of tumors.

Key words: chemotherapy, fetal rhabdomyomatous nephroblastoma, Wilms' tumor, Wilms' tumor suppressor gene

Wilms' tumor (WT) is the most common malignant neoplasm of the kidney in childhood, accounting for approximately 8% of all childhood solid tumors, and 5–10% of WT patients present with bilateral disease.[1,2] Pathologically, bilateral WT tends to be fetal rhabdomyomatous nephroblastoma (FRN), a histological variant of WT characterized by a predominance of rhabdomyogenic components. Clinically, WT of the FRN type presents as a huge mass in younger patients. The tumor rarely metastasizes or shows aggressive behavior, and it has a good prognosis.[3] On the other hand, FRN is known to be resistant to the chemotherapy used to treat classical WT.[4,5] The Wilms' tumor suppressor gene (*WT1*) at chromosome 11p13 was identified in 1990, and it encodes a transcriptional factor containing a domain of four zinc finger motifs.[6,7] Schumacher *et al.* reported finding *WT1* mutations in four of the five cases of bilateral WT that they analyzed,[8] a much higher incidence than in sporadic WT.[1,2] Bilateral WT is explained by the two-hit mechanism of inactivation of tumor suppressor genes proposed by Knudson and Strong.[8–10] Because a germ line mutation in *WT1* has been reported to predispose the development of tumors with stromal-predominant histology,[8] the *WT1* mutation should be found in bilateral WT, especially the FRN histological subtype. However, there have been no reports discussing correlations between the histology of WT, the chemotherapy response and *WT1* mutations.

This report summarizes the clinical and pathological features in five cases of bilateral WT. This study analyzed the *WT1* gene mutation and attempted to determine why they are resistant to chemotherapy.

MATERIALS AND METHODS

Patients

Five patients with bilateral WT who underwent surgery between 1998 and 2001 were studied. Cases 2–5 were accompanied by genitourinary tract malformations (Table 1).

Correspondence: Jun-ichi Hata, MD, National Research Institute for Child Health and Development, 3-35-31 Taishido, Setagaya-ku, Tokyo 154-8567, Japan. Email: jhata@nch.go.jp

Received 19 September 2002. Accepted for publication 6 December 2002.

Table 1 Clinical and histological features and results of *WT1* mutations

Case	Age/Sex	Anomaly	Histology before chemotherapy	First chemotherapy	Tumor volume after therapy	Histological subtype after chemotherapy	Mutations germ line	Mutations tumor	Outcome
1	9 months/F	–	Epithelial type	V+A	Decrease	Epithelial type	–	–	Disease-free postoperative status
2	11 months/M	Cryptorchidism	FRN	V+A+D†	Increase	FRN	1168C→C/T	1168X→T(R390X)	Disease-free postoperative status
3	9 months/F	Cryptorchidism hypospadias	Nephroblastic-type striated muscle (+)	V+A†	Regression (-)	FRN	1168C→C/T	1168X→T(R390X)	Disease-free postoperative status
4	7 months/F	Ovarian dysgenesis	FRN	V+A†	Increase	FRN	1168C→C/T	1168X→T(R390X)	Disease-free postoperative status
5	1 year/M	Cryptorchidism	Nephroblastic-type striated muscle (+)	V+A†	Increase	Nephroblastic-type striated muscle cells: increase	1168C→C/T	1168X→T(R390X)	Under treatment

†Additional aggressive chemotherapy was performed. A, actinomycin; C, cytosine; D, doxorubicin; FRN, fetal rhabdomyomatous nephroblastoma; T, thymine; V, vincristine.

Cases 2 and 5 were associated with cryptorchidism, case 3 with bilateral cryptorchidism and hypospadias, and case 4 with left ovarian dysgenesis. None of the patients showed evidence of renal dysfunction or renal failure. Fresh tumor tissue and peripheral blood samples were obtained from all five patients when tumorectomy was performed. The clinical features of the patients are summarized in Table 1. Informed consent was obtained from all patients or their parents.

Histopathological analysis

The biopsy specimens before chemotherapy and the resected tumors after chemotherapy were fixed with 10% formalin and embedded in paraffin. Paraffin sections were stained with H&E. Histological subtyping of WT was performed according to the classification proposed by the Japanese Society of Pathology, [11] and FRN was defined as more than 1/3 of the tumor mass showing striated muscle differentiation. However, the nephroblastic type of tumor was defined as the tumor that showed triphasic histology containing striated muscle, but its proportion of the tumor was less than 1/3.[11] We used biopsied specimens to diagnose the histology of tumors before chemotherapy. All five cases underwent open biopsy and we took them to represent the histology of tumor. Some sections were subjected to immunohistochemistry for WT1, Ki-67, myogenin and S-100 protein by the avidin-biotin-peroxidase technique using anti-WT1 antibody (dilution 1:200; DAKO, Carpinteria, CA, USA), anti-Ki-67 antibody (dilution 1:500; DAKO, Kyoto, Japan), antimyogenin antibody (dilution 1:200; Santa Cruz, CA, USA) and anti-S-100 protein antibody (dilution 1:2000; DAKO, Japan). For WT1 staining, deparaffinized and rehydrated sections were treated with 0.4% pepsin in 0.2 NHCl for 30 min at 37°C before reacting with anti-WT1 antibody. Deparaffinized and rehydrated sections were heated at 100°C in 0.01 mol/L sodium citrate buffer (pH 6.0) for 10 min before reacting with anti-Ki-67 and antimyogenin antibody.

DNA preparation

The DNA was extracted from leukocytes and tumor tissue by the sodium dodecyl sulfate-proteinase K method with slight modifications, as described previously.[12] Amplification of exons 1–10 was performed by polymerase chain reaction (PCR). Direct sequencing of the PCR products was performed with a MegaBACE 1000 DNA Sequencing System (Amersham Biosciences, Florida, USA). The precise methods have been described previously.[12] The PCR and sequence primers we used are shown in Table 2. All procedures were approved by the Ethical Committee of the Keio University School of Medicine.

Table 2 Polymerase chain reaction (PCR) and sequence primers

exon	Name	PCR sequence	Name	Sequence
1	WT256	AGCCAGAGCAGCAGGGAGTC	SEQ1-S	GGCATCTGGGCCAAGTTAGG
	WTEX1R2	CGGTCAAAAGGGGTAGGAGA	SEQ1-A	CCTAGAGCGGAGAGTCCCTG
2	2B-S	TGGCTGGTTCAGACCCACTG	SEQ2-S	TGCCCCGTCTTGCGAGAGCA
	2B-A	AGAGGAGGATAGCACGGAAG	SEQ2-A	GCACGGAAGAAGGGGAGAAG
3	3B-S	CCAGGCTCAGGATCTCGTGT	SEQ3-S	ATCTCGTGTCTCCCCCAACC
	3B-A	GGCGTCTCGTGCCTCCAAGA	SEQ3-A	GTGCCTCCAACACCCTGCAT
4	4B-S	TGTGGAGGCTTGCACTTTCA	SEQ4-S	GAAGAAACAGTTGTGTATTATTTTG
	4B-A	GCCCTTTCTTCTAAAACTGT	SEQ4-A	ATGGTTCAAACAGGTATAAGTTACT
5	5B-S	TCACTGGATTCTGGGATCTG	SEQ5-S	CTGGGATCTGGGGGGCTTGCCA
	5B-A	AGTCCTAACTCCTGCATTGC	SEQ5-A	CCCCAGGTGCCAGTCAGCAAGG
6	6B-S	AAAACCATCATTCCCTCCTG	SEQ6-S	TTTCCAAATGGCGACTGTGAGC
	6B-A	CAAAGAGTCCATCAGTAAGG	SEQ6-A	GGTAAGTAGGAAGAGGCAGTGC
7	7F-S	GTGCTCACTCTCCCTCAAGA	SEQ7-S	TCCCTCAAGACCTACGTGAATGTTC
	7F-A	GTGAGAGCCTGGAAAAGGAGC	SEQ7-A	TTGAACCATGTTTGCCCAAGACTGG
8	8-S	AGATCCCCTTTTCCAGTATC	SEQ8-S	AGATCCCCTTTTCCAGTATC
	8C'-A	CAACAACAAAGAGAATCA	SEQ8-A	AAATCAACCCTAGCCCAAGG
9	9C-S	AAGTCAGCCTTGTGGGCCTC	SEQ9-S	CCCACATTGGTTAGGGCCGAGGCTA
	9C-A	TTTCCAATCCCCTCTCATCAC	SEQ9-A	TAGGGCCGAGGCTAGACCTTCTCT
10	10C-S	CACTCGGGCCTTGATAGTTG	SEQ10-S	TTTCCAATCCCCTCTCATCAC
	10C-A	GTCAGACTTGAAAGCAGTTC	SEQ10-A	TGTGCCTGTCTCTTTGTTGC

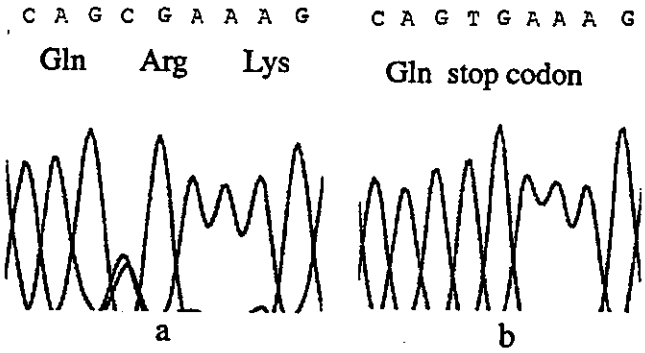

Figure 1 Results of the DNA sequence analyses of germ line (a) and tumor samples (b). (a) A heterozygous point mutation, 1168 cytosine/thymine, was found in exon 9 in the germ line in cases 2–5. (b) A point mutation, 1168C/T, converts the codon for 390Arg into a stop codon in the tumors in cases 2–5.

RESULTS

The clinical and pathological features and results of *WT1* mutations are summarized in Table 1. The DNA sequence analyses indicated the same point mutations at exon 9 in cases 2–5. The mutation was a cytosine to a thymine substitution in zing finger 3 and resulted in a ^{390}Arg becoming a stop codon (R390X). There was a heterozygous mutation at the same codon in the germ line of all four patients (Fig. 1). No *WT1* mutation was detected in case 1.

The histological subtype in case 1 was the epithelial type, and the specimens before chemotherapy contained no clear striated muscle components. Cases 2 and 4 showed the typical histological features of FRN. Cases 3 and 5 were nephroblastic type and contained abundant striated muscle components before chemotherapy.

Only case 1 was responsive to chemotherapy consisting of vincristine and actinomycin D. As the tumor volume in the other cases either increased (cases 2, 4, and 5) or was unchanged (case 3), additional aggressive chemotherapy was carried out in these four cases, but tumor regression did not occur regardless of the chemotherapy regimen. Finally, all patients underwent bilateral tumorectomy. Cases 1–4 are disease-free after tumorectomy. In case 5, tumor rupture occurred during chemotherapy, and the patient is now on chemotherapy after bilateral nephrectomy.

Histological examination of all resected tumors after chemotherapy, except in case 1, showed a predominance of mature striated muscle and collagenous tissue (Fig. 2). The epithelial and blastemal components of cases 2–5 were markedly reduced in the tumor tissue. However, we diagnosed case 3 as nephroblastic type before chemotherapy because almost the entire tumor was composed of striated muscle components after chemotherapy. Therefore, we diagnosed case 3 as an FRN-like tumor after chemotherapy. The resected tumor of case 1 contained no striated muscle or collagen fibers. None of the tumors examined showed histological anaplasia before or after chemotherapy.

Before chemotherapy, the striated muscle cells were positive for myogenin, a protein that regulates the differentiatin of myogenic cells and is expressed in the cells induced to differentiate (Fig. 3a), and they were negative for S-100 protein, which is expressed in mature skeletal muscles (Fig. 3b). After chemotherapy, mature striated muscle was negative for myogenin (Fig. 3c) and positive for S-100 protein (Fig. 3d). Ki-67 was positive in the nuclei of almost all of the tumor cells

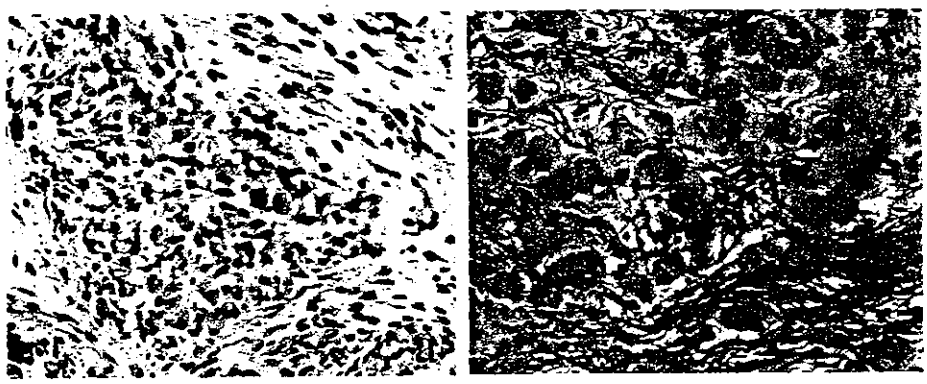

Figure 2 H&E section from case 4. (a) Preoperative biopsy. Immature striated muscle is the predominant stromal element. (original magnification, ×100) (b) Resected tumor after chemotherapy. The components are mostly mature striated muscle and collagen fiber. (original magnification, ×100)

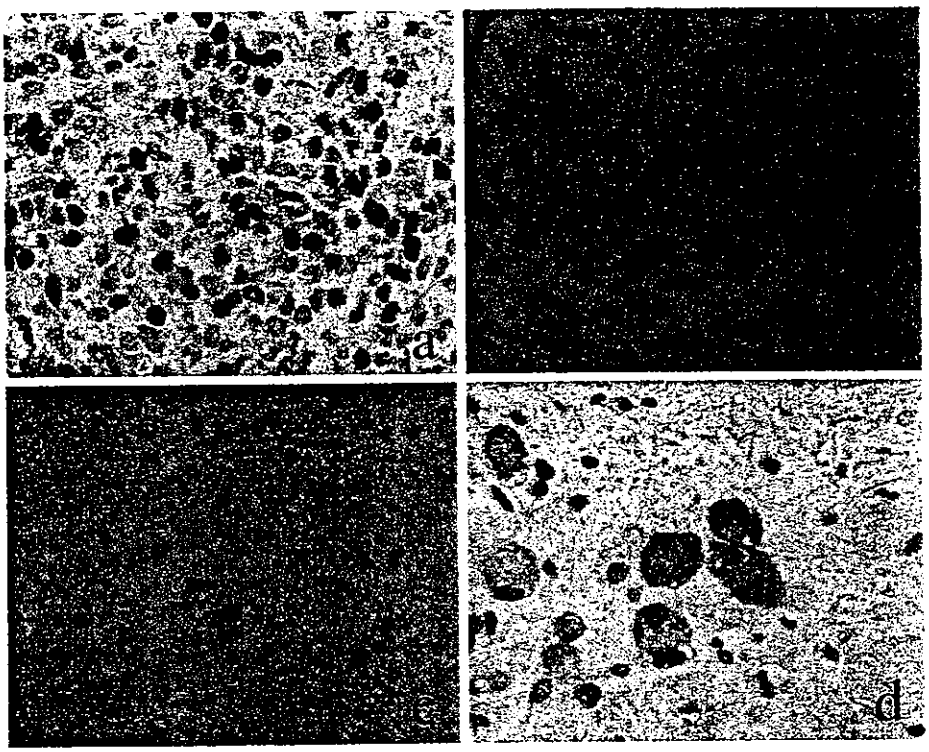

Figure 3 Immunohistochemical analysis of sections from case 4 with myogenin and S-100 protein (original magnification, ×200) (a) Striated muscle cells before chemotherapy are positive for myogenin, a protein that regulates myogeninc cell differentiation and is expressed in cells induced to differentiate. (b) Tumor cells before chemotherapy are negative for S-100 protein, expressed in mature skeletal muscle. (c) Striated muscle cells after chemotherapy are negative for myogenin. (d) Striated muscle cells after chemotherapy are positive for S-100 protein.

before chemotherapy (Fig. 4a), but the mature striated muscle cell components were almost negative for Ki-67 (Fig. 4b). The epithelial and blastemal components of the tumors were positive for Ki-67 (data not shown). The tumors in cases 2–5 that carried the *WT1* point mutation were negative for *WT1* staining (Fig. 5a), whereas case 1, which did not have the *WT1* mutation, was positive for immunostaining (Fig. 5c).

DISCUSSION

In this report, we have summarized the clinical course and histological features in five cases of bilateral WT before and after chemotherapy. We also demonstrated a *WT1* mutation in them. Our results support that loss of *WT1* expression as a result of *WT1* mutation is correlated with the histological features of WT.[8] They also suggest that histological features are related to the response of chemotherapy. As unilateral WTs are usually resected before chemotherapy according to the Japan Wilms' Study Group protocol, it is difficult to compare histological features before and after chemotherapy. The estimated incidence of *WT1* mutation in unilateral or sporadic WT cases is approximately 10–15%.[2] We consider it important to clarify the histological features and response to chemotherapy in bilateral WTs carrying *WT1* mutations with higher incidence than unilateral WTs.

Cases 2–5 were found to have the same point mutations, a change from C to T in zing finger 3, resulting in ^{390}Arg becoming a stop codon. During translation, this nonsense mutation leads to protein truncation, with the result that the last zing finger necessary for DNA binding of *WT1* is missing. Interrupted DNA binding to the target genes of *WT1* fusion

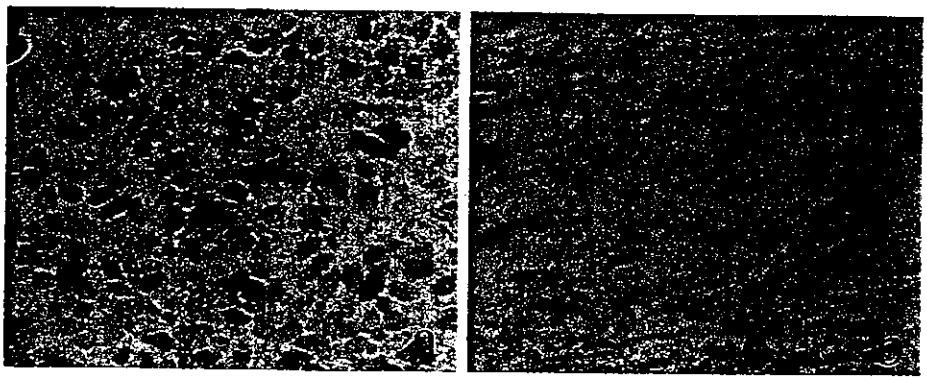

Figure 4 Immunohistochemical analysis of Ki-67 (original magnification, ×400) (a) Preoperative biopsy of Case 3. Tumor cells are positive for Ki-67 before chemotherapy. (b) Resected tumor of case 3. Tumor tissue is negative for Ki-67.

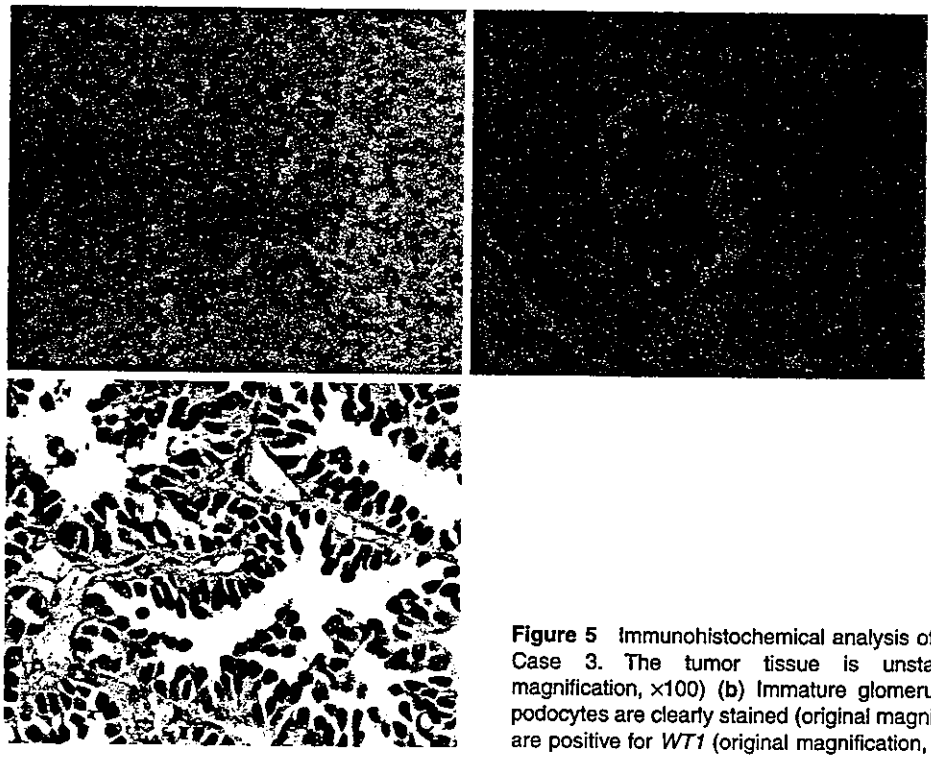

Figure 5 Immunohistochemical analysis of Wilms' tumor suppressor gene (*WT1*). (a) Case 3. The tumor tissue is unstained by anti-*WT1* antibody (original magnification, ×100) (b) Immature glomerulus in the same section of case 3. The podocytes are clearly stained (original magnification, ×400) (c). Case 1. The tumor cells are positive for *WT1* (original magnification, ×400).

proteins with loss of the last zing finger have been previously demonstrated by electrophoretic mobility shift assays.[13] There was a heterozygous mutation at the same point in the germ line of all four patients, thereby supporting the two-hit mutational model of bilateral WT.

In earlier studies, mutation R390X had been found in patients with sporadic unilateral WT, in a patient with bilateral WT, and in a patient with WT associated with urogenital malformation.[14] This mutation has also been detected in a patient with acute promylocytic leukemia[15] and a patient with an isolated genital malformation without WT.[16] Although the histological findings in the WTs with the R390X mutation were not described in the literature, from our results, this R390X mutation might correlate with rhabdomyomatous histology in bilateral WT.

The cases with *WT1* mutation immunohistochemically stained negative for WT1. Loss of *WT1* function has been reported to be the underlying cause of tumor development.[8] Miyagawa *et al.* reported that loss of *WT1* function leads to ectopic myogenesis in WT, and suggested that normal expression of WT1 might prevent the metanephric-mesenchymal stem cells of the kidney from differentiating into skeletal muscle.[17] All four cases had *WT1* mutations, and cases 2 and 4 showed stromal-predominant histology. Cases 3 and 5 showed the nephroblastic type before chemotherapy, and it could not be concluded that all WTs with the R390X mutation present with FRN histologically. Cases 3 and 5 contained skeletal muscle cells as a stromal component. After chemotherapy, case 3 showed FRN and case 5 had more striated muscle cells than before chemotherapy. All

four cases were negative for *WT1*. Loss of *WT1* expression is related to histological features, at least in bilateral WT.

Tumor volume, except for case 1, increased or failed to regress after the usual chemotherapy for classical WT, and the tumors appeared to be resistant to the usual chemotherapy. Histologically, all tumors, except case 1, showed a marked predominance of mature striated muscle, including increased collagen fibers and decreased epithelial and blastemal components, after chemotherapy. Before chemotherapy, all tumor components, stromal, epithelial, and blastemic, were strongly positive for Ki-67, a cell proliferation-related antigen absent in the G0 phase. After chemotherapy,striated muscle, which was the main component of the tumors, was negative for Ki-67. Tubular structures and blastema were positive for Ki-67, but they were a very small component of the tumors. Further, FRN been reported to be a poor responder to preoperative chemotherapy,[4,5] and Anderson *et al.* reported that rhabdomyomatous histology in bilateral Wilms' tumors is associated with poor response to chemotherapy.[18] Except for case 1, tumor volume in either increased or failed to regress after chemotherapy. Histologically, however, the immature component decreased and the mature component increased. The mature component showed less proliferate activity. Apparently, chemotherapy was effective, but tumor volume did not decrease because of the increase in collagen fibers. Most clinicians assume that chemotherapy is ineffective if tumor volume does not change after chemotherapy, and they consider continuous or additional chemotherapy. Additional aggressive chemotherapy consisting of etoposide, carboplatin and cyclophosphamide, which is said to be effective against proliferating tumor cells, was performed in our cases. These anticancer drugs are ineffective against tumors mainly composed of mature striated muscle components. The prognosis of FRN has been said to be good,[3,4] and our four cases have been free of disease since tumor resection. Aggressive chemotherapy, which has little effect on the tumor and might cause complications, should be avoided. The usual chemotherapy for the stage in each side is sufficient. However, there might be residual immature components that show proliferative activity and have the potential to metastasize. Surgical resection of tumors after usual chemotherapy is essential.

Nagashima *et al.* reported myogenic differentiation of stromal cells in the nude mouse WT line.[19] Wilms' tumor tends to spontaneously differentiate into mature elements, although it is not as well known as neuroblastoma. Zuppan *et al.* reported differentiation of WT after preoperative chemotherapy.[20] Seenmayer *et al.* and Ishikawa *et al.* reported a case of WT in which complete maturation of a pulmonary metastasis was documented after chemotherapy.[21,22] Chemotherapy might induce mesenchymal differentiation in WT and promote tumor maturation. The results clearly indicate that immature stromal components in our cases differentiated into mature striated muscles. This maturation is probably attributable to both the inherent nature of WT to differentiate and the effect of chemotherapy.

The histological diagnosis before therapy is important when deciding the management of bilateral WT. If the diagnosis is FRN, chemotherapy could not be expected to result in tumor reduction. Tumors might be resected in the early course of the therapy, for example, after one course of chemotherapy or before chemotherapy, if renal preservation is possible.

In conclusion, the histological features strongly correlate with *WT1* mutation in bilateral WT. Preoperative diagnostic biopsy is important in bilateral WT because if the pathological subtype of the tumor is FRN or it contains striated muscle, tumor volume reduction cannot be the expected response to chemotherapy, even if chemotherapy is effective. Clarification of the biological characteristics of bilateral WT is required in order to determine the most suitable treatment.

ACKNOWLEDGMENTS

We thank Drs H. Horie (Chiba Children's Hospital), K. Hashizume and Y. Kanamori (University of Tokyo Faculty of Medicine), J. Miyauchi and Y. Tsunematsu (National Center for Child Health and Development), Y. Hayashi (Tohoku University School of Medicine) and Y. Ogawa (Saitama Childrenís Medical Center) for providing samples and clinical data. We thank Mr H. Suzuki for his technical assistance.

This work was supported by a Grant-in-Aid for Scientific Research from the Ministry of Education, Culture, Sports, Science and Technology (11557021, 13470053, 13022264 and 11167274), as well as a Cancer Research Grants from the Ministry of Health, Labor and Welfare (9–14, 10D-1).

REFERENCES

1 Coppes MJ, Pritchard-Jones K. Principles of Wilms' tumor biology. *Urol Clin North Am* 2000; **27**: 423–33.
2 Lee SB, Haber DA. Wilms' tumor and the WT1 gene. *Exp Cell Res* 2001; **264**: 74–99.
3 Wigger HJ. Fetal rhabdomyomatous nephroblastoma-a variant of Wilms' tumor. *Hum Pathol* 1976; **7**: 613–23.
4 Maes P, Delemarre J, de Kraker J, Ninane J. Fetal rhabdomyomatous nephroblastoma: a tumour of good prognosis but resistant to chemotherapy. *Eur J Cancer* 1999; **35**: 1356–60.
5 Saba LM, de Camargo B, Gabriel-Arana M. Experience with six children with fetal rhabdomyomatous nephroblastoma: review of the clinical, biologic, and pathologic features. *Med Pediatr Oncol* 1998; **30**: 152–5.
6 Call KM, Glaser T, Ito CY *et al.* Isolation and characterization of a zinc finger polypeptide gene at the human chromosome 11 Wilms' tumor locus. *Cell* 1990; **60**: 509–20.
7 Gessler M, Poustka A, Cavenee W *et al.* Homozygous deletion in Wilms tumours of a zinc-finger gene identified by chromosome jumping. *Nature* 1990; **343**: 774–8.

8 Schumacher V, Schneider S, Figge A *et al.* Correlation of germline mutations and two-hit inactivation of the WT1 gene with Wilms tumors of stromal-predominant histology. *Proc Natl Acad Sci USA* 1997; **94**: 3972–7.
9 Huff V, Miwa H, Haber DA *et al.* Evidence for WT1 as a Wilms tumor (WT) gene: intragenic germinal deletion in bilateral WT. *Am J Hum Genet* 1991; **48**: 997–1003.
10 Knudson AG Jr, Strong LC. Mutation and cancer: a model for Wilms' tumor of the kidney. *J Natl Cancer Inst* 1972; **48**: 313–24.
11 Committee on histological classification of childhood tumors the Japanese pathological society. Histological classification and atlas of tumors in infancy and childhood I T Tumors of the urinary system. In: Urano Y, ed. *Tumors of the Kidneys*. Tokyo: Kanehara, 1988; 12–3.
12 Takata A, Kikuchi H, Fukuzawa R, Ito S, Honda M, Hata J. Constitutional WT1 correlate with clinical features in children with progressive nephropathy. *J Med Genet* 2000; **37**: 698–701.
13 Little M, Holmes G, Bickmore W, van Heyningen V, Hastie N, Wainwright B. DNA binding capacity of the WT1 protein is abolished by Denys–Drash syndrome WT1 point mutations. *Hum Mol Genet* 1995; **4**: 351–8.
14 Little M, Wells C. A clinical overview of WT1 gene mutations. *Hum Mutat* 1997; **9**: 209–25.
15 King-Underwood L, Renshaw J, Pritchard-Jones K. Mutations in the Wilms' tumor gene WT1 in leukemias. *Blood* 1996; **87**: 2171–9.
16 Kohler B, Schumacher V, l'Allemand D, Royer-Pokora B, Grutters A. Germline Wilms tumor suppressor gene (WT1) mutation leading to isolated genital malformation without Wilms tumor or nephropathy. *J Pediatr* 2001; **138**: 421–4.
17 Miyagawa K, Kent J, Moore A *et al.* Loss of WT1 function leads to ectopic myogenesis in Wilms' tumour. *Nat Genet* 1998; **18**: 15–7.
18 Anderson J, Slater O, McHigh K, Duffy P, Pritchard J. Response without shrinkage in bilateral Wilms tumors: Significance of rhabdomyomatous histology. *J Pediatr Hematol Oncol* 2002; **24**: 31–4.
19 Nagashima Y, Nishihira H, Miyagi Y *et al.* A nude mouse Wilms' tumor line (KCMC-WT-1) derived from an aniridia patient with monoalleleic partial deletion of chromosome 11p. *Cancer* 1996; **77**: 799–804.
20 Zuppan CW, Beckwith JB, Weeks DA, Luckey DW, Pringle KC. The effect of preoperative therapy on the histologic features of Wilms' tumor. An analysis of cases from the Third National Wilms' Tumor Study. *Cancer* 1991; **68**: 385–94.
21 Seemayer TA, Harper JL, Shickell D *et al.* Cytodifferentiation of a Wilms' tumor pulmonary metastasis: theoretic and clinical implications. *Cancer* 1997; **79**: 1629–34.
22 Ishikawa K, Toyoda Y, Fukuzato Y, Kato K, Ijiri R, Tanaka Y. Maturation in the primary and metastatic lesions of fetal rhabdomyomatous nephroblastoma. *Med Pediatr Oncol* 2001; **37**: 62–3.

Pathology International 2003; 53: 106–110

Case Report

Primary carcinosarcoma of the vagina

Rie Shibata,[1] Akihiro Umezawa,[1] Kyoko Takehara,[2] Daisuke Aoki,[2] Shiro Nozawa[2] and Jun-ichi Hata[1,3]

Departments of [1]Pathology and [2]Obstetrics and Gynecology, Keio University School of Medicine, and [3]National Research Institute for Child Health and Development, Tokyo, Japan

Primary carcinosarcoma of the vagina is a very rare tumor, with only eight cases diagnosed as carcinosarcoma in the literature that we are aware of. We recently encountered a case of primary carcinosarcoma of the vagina in a 75-year-old woman. The patient had a history of hysterectomy and bilateral ovariectomy for uterine corpus cancer at 55 years of age. Recurrence of the cancer was suspected 17 years after the operation and irradiation therapy was performed, but the patient died 3 years after the recurrence. Autopsy revealed a mass lesion in the pelvic cavity that originated in the vagina. Histological examination showed that the tumor contained anaplastic carcinoma, rhabdomyosarcoma, leiomyosarcoma and chondrosarcoma components, and it was diagnosed as carcinosarcoma. The histological diagnosis of the uterine corpus cancer was well-differentiated adenocarcinoma, and there was no sarcomatous component. The carcinosarcoma occurred 17 years after the hysterectomy, and it was concluded to be a primary carcinosarcoma of the vagina. This is the first case of primary vaginal carcinosarcoma in which the epithelial and sarcomatous components were clearly identified histologically and immunohistochemically.

Key words: carcinosarcoma, malignant mixed mullelian tumor, vagina.

Carcinosarcomas (malignant mixed mullerian tumors) of the female genital tract are highly aggressive neoplasms characterized by mixture of malignant epithelial and stromal elements. Carcinosarcoma of the uterine corpus is well known, but it accounts for only 2–3% of all malignant tumors of the uterus.[1] Primary carcinosarcoma of the vagina is a very rare tumor, and there are only a few reports of cases diagnosed as carcinosarcoma or malignant mixed mullerian tumor of vaginal origin in the literature.[2–6] We report here a case of primary carcinosarcoma of the vagina that occurred in a 75-year-old woman.

Correspondence: Jun-ichi Hata, National Research Institute for Child Health and Development, 3-35-31 Taishido Setagaya-ku, Tokyo 154-8567, Japan. Email: jhata@nch.go.jp

Received 5 July 2002. Accepted for publication 13 September 2002.

CLINICAL SUMMARY

The patient had a history of hysterectomy and bilateral ovariectomy for cancer of the uterine corpus at age 55 years. The tumor was localized in the uterine corpus and showed deep myometrial invasion. It was diagnosed as stage Ic. The histological diagnosis was well-differentiated adenocarcinoma (Fig. 1a). A mass lesion was detected in the pelvic cavity 17 years after the operation and recurrence of the uterine corpus cancer was suspected. Para-aortic lymph node metastasis was also detected. Biopsy specimen of the tumor lesion at the vagina was diagnosed as poorly differentiated adenocarcinoma (Fig. 1b). Pelvic irradiation therapy was performed, but the patient died 3 years after the recurrence was suspected aged 75 years.

PATHOLOGICAL FINDINGS

At autopsy, the tumor was found to have originated in the vagina, directly invading the bladder, and formed a mass lesion in the pelvic cavity. The mass had compressed both ureters, causing hydronephrosis and hydroureter. Bone metastasis and a para-aortic lymph node metastasis were also diagnosed. The para-aortic lymph node to which the tumor had metastasized measured 15 × 9.5 × 11 cm. Its cut surface was white to yellow-white, and necrosis and hemorrhage were observed (Fig. 2).

Histological examination of the pelvic mass lesion at autopsy revealed mainly anaplastic carcinoma (Fig. 3a). The tumor cells contained bizarre nuclei and exhibited high mitotic activity. A small rhabdomyosarcoma component, which was positive for myoglobin (data not shown), was present. Squamous epithelium of the vagina could not be identified because of degenerative changes and necrosis. The metastatic lesion of the para-aortic lymph node contained components consistent with rhabdomyosarcoma (Fig. 4b), leiomyosarcoma (Fig. 4c) and chondrosarcoma (Fig. 4d) as well as anaplastic carcinoma. The metastatic lesion of the bone contained a chondrosarcoma component.

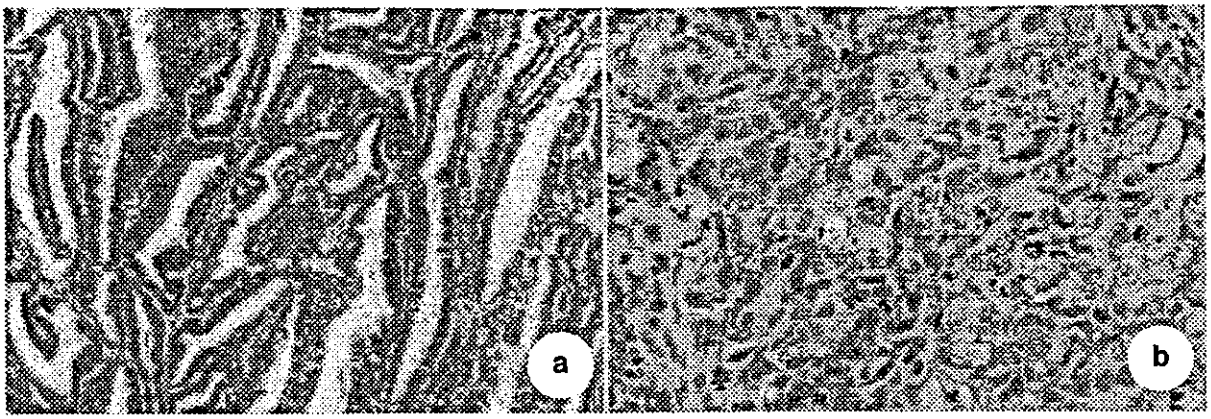

Figure 1 Histological appearance of the uterine corpus cancer at 55 years and the biopsy specimen of the vagina when the pelvic mass was detected 17 years later. (a) The histological diagnosis of the uterine corpus cancer was well-differentiated adenocarcinoma and no sarcomatous components were seen. The tumor cells had a glandular pattern and exhibited papillary growth. (H&E, original magnification ×40) (b) Biopsy specimen of the vagina. The tumor cells had atypical nuclei and proliferated without a glandular pattern. (H&E, original magnification ×200)

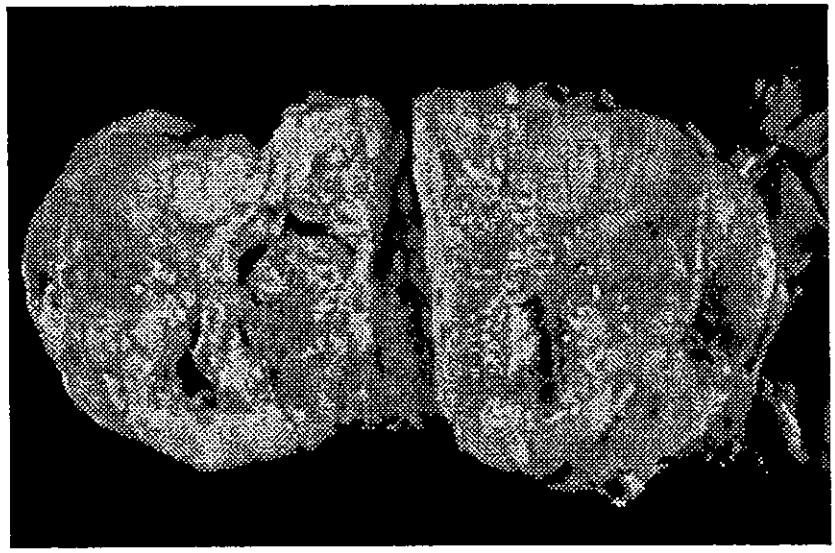

Figure 2 Cut surface of the paraaortic lymph node to which the carcinosarcoma had metastasized. The node measured 15 × 9.5 × 11 cm, and its cut surface was yellow-white in color. The lesion was mainly composed of solid and soft parts, but there were also hard foci. Necrosis and hemorrhage were seen.

Immunohistochemical results are summarized in Table 1. The tumor cells of the anaplastic carcinoma component were positive for broad-spectrum cytokeratin (Fig. 4a). The tumor cells of the rhabdomyosarcoma component were positive for myoglobin (Fig. 4b), the tumor cells of the leiomyosarcoma component were positive for smooth muscle actin (Fig. 4c), and the tumor cells of the chondrosarcoma component were positive for S-100 protein (Fig. 4d). All the tumor cells were negative for neuron-specific enolase, chromogranin and synaptophysin (data not shown).

DISCUSSION

Primary vaginal carcinosarcoma is a very rare tumor, and only eight cases have been reported in the literature.[2-6] Seven cases were in review articles on female genital tract malignancies, but histological and immunohistochemical information on each case was not described in the literature.[2,3,5,6] Neesham *et al.* reported one case of homologous vaginal carcinosarcoma[4] without a detailed account of the immunohistochemical study. Our case is the first case in

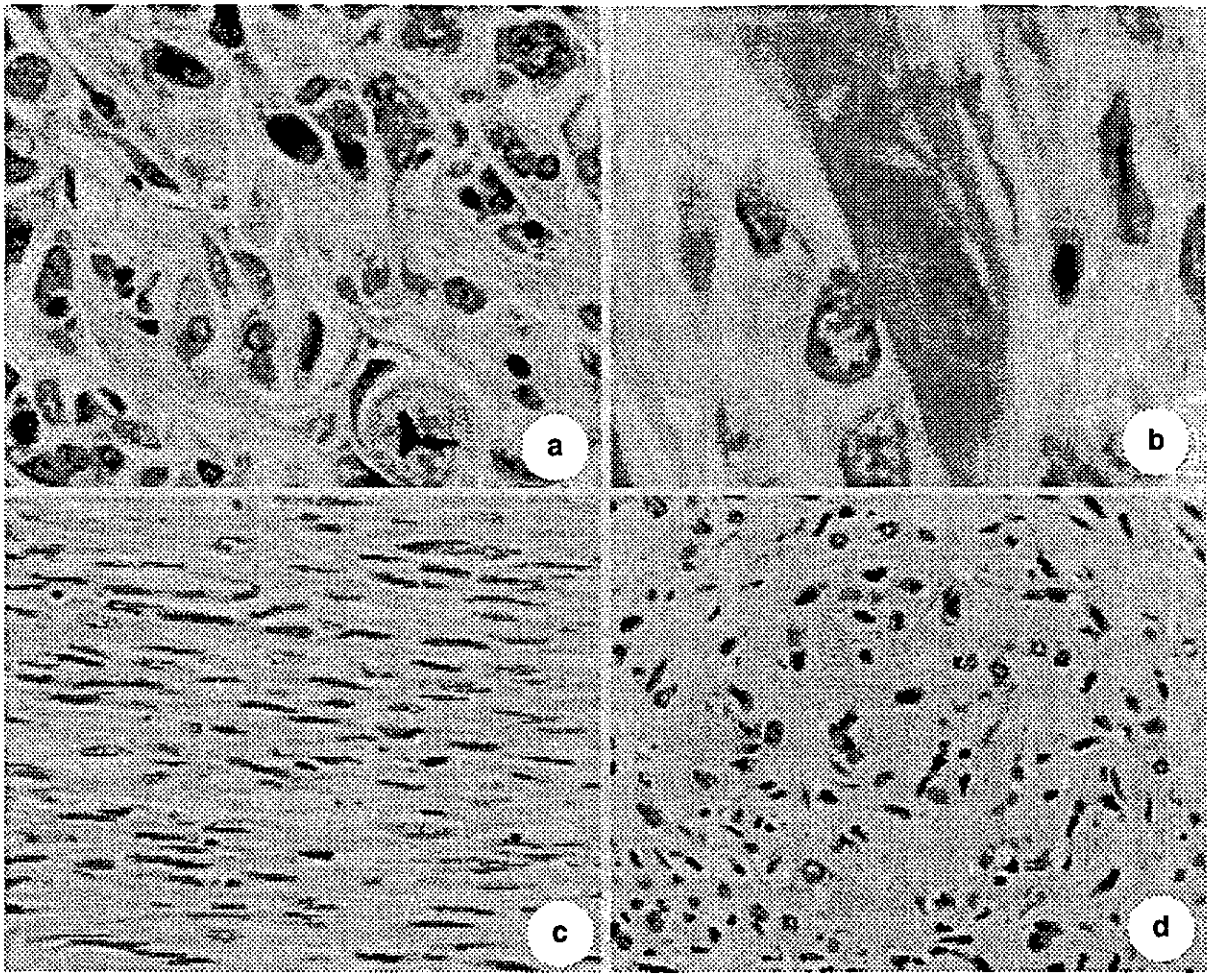

Figure 3 The epithelial and sarcomatous components of carcinosarcoma. (H&E) (a) Anaplastic carcinoma. Tumor cells with bizarre nuclei proliferated and atypical mitoses were seen (original magnification x200) (b) Rhabdomyosarcoma. Tumor cell showed striated structure (original magnification x400) (c) Leiomyosarcoma. Tumor cells with spindle-shaped cytoplasm were seen (original magnification x200) (d) Chondrosarcoma. The tumor components formed hyaline cartilage (original magnification x200).

which epithelial and sarcomatous components have been clearly identified histologically and immunohistochemically. The patient was diagnosed with uterine corpus cancer 20 years before she died, and the histological diagnosis was well-differentiated adenocarcinoma with no sarcomatous component. A pelvic mass was detected 17 years after the hysterectomy, and a biopsy specimen of the vagina was diagnosed as poorly differentiated adenocarcinoma. At first, the tumor was thought to be a recurrence of the adenocarcinoma diagnosed 17 years previously, but at autopsy, the pelvic tumor was found to have originated in the vagina and to be a carcinosarcoma. The biopsy specimen of the vagina 3 years before the patient's death did not represent a recurrence of the adenocarcinoma, but the epithelial component of the carcinosarcoma contained a different neoplasm. As the patient had undergone hysterectomy and bilateral ovariectomy, the carcinosarcoma definitely arose in the vagina.

Recent studies have suggested the combination tumor theory to explain the histogenesis of gynecologic carcinosarcoma.[7,8] Although vaginal carcinosarcoma was not included among the cases, as the proximal portion of the vagina is derived from the mullerian duct, the histogenesis of vaginal carcinosarcomas is thought to be the same as that of uterine carcinosarcomas. Sreenan *et al.* suggested the so-called conversion theory, which could be regarded as a variant of the combination theory.[9] They concluded that the dominant element in carcinosarcomas of the female genital tract is the epithelial component, and sarcomatous components evolve from the carcinoma as a secondary phenomenon. Our case received irradiation therapy after carcinoma of the vagina

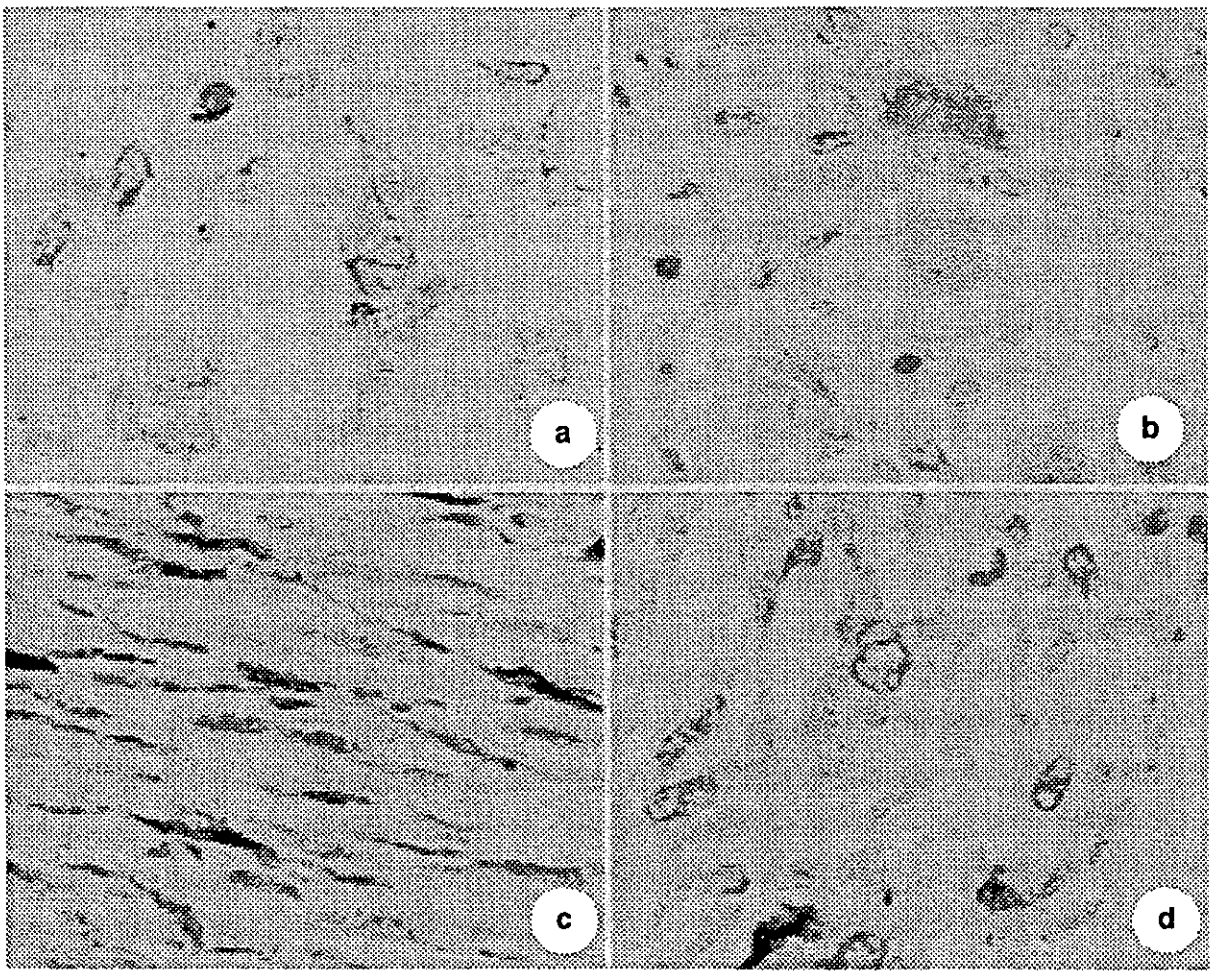

Figure 4 Immunohistochemical analysis of the carcinosarcoma (original magnification ×200). (a) The anaplastic carcinoma component is positive for broad-spectrum cytokeratin. (b) The rhabdomyosarcoma component is positive for myoglobin. (c) The leiomyosarcoma component is positive for smooth-muscle actin. (d) The chondrosarcoma component is positive for S-100 protein.

Table 1 Results of immunohistochemical staining

Antigen	Source	Dilution	Carcinoma	Rhabdomyosarcoma	Leiomyosarcoma	Chondrosarcoma
Broad-spectrum cytokeratin	Dako, Kyoto, Japan	1:100	Positive	Negative	Negative	Negative
Myoglobin	Santa Cruz, CA, USA	1:200	Negative	Positive	Negative	Negative
Smooth-muscle action	Santa Cruz	1:100	Negative	Negative	Positive	Negative
S-100	Santa Cruz	1:200	Negative	Negative	Negative	Positive
Neuron-specific enolase	Biogenex, CA, USA	1:2000	Negative	Negative	Negative	Negative
Chromogranin A	Dako	1:200	Negative	Negative	Negative	Negative
Synaptophysin	Dako	1:20	Negative	Negative	Negative	Negative

was detected. It might be possible that irradiation influenced the conversion of carcinoma to sarcoma. Further investigation on the histological changes of carcinosarcomas after irradiation therapy to determine the histogenesis of carcinosarcomas is required.

An association between carcinosarcoma and previous irradiation of the pelvic cavity has been well established.[10] Irradiation therapy was performed in our patient, but it was after development of the carcinosarcoma and the uterine corpus cancer had been treated by surgical resection of uterus and ovaries. Therefore, the patient had no history of chemotherapy or irradiation therapy. The relationship between the adenocarcinoma of uterine corpus and carcinosarcoma of vagina is unclear.

The 5-year survival rate for vaginal carcinosarcoma has been reported to be 17%,[5] and only one case of 5-year survival without disease has been reported.[2] The prognosis of uterine corpus carcinosarocma is also poor, and the reported 5-year survival rate is 18–39%. The outcome of metastatic carcinosarcomas is extremely poor, and Colombi reported that patients died within 1 year of diagnosis.[11] However, some patients with metastatic carcinosarcoma survived for 3–4 years.[9] The prognosis of metastatic carcinosarcoma might differ according to its origin and metastatic site at the time of initial diagnosis. Although irradiation therapy was used to treat our patient, she died 3 years after the tumor was detected. Aggressive therapy, including surgical resection, irradiation therapy and chemotherapy, is required to cure the tumor. Further research is required in order to determine appropriate treatment and evaluate the outcome of this rare type of tumor.

REFERENCES

1 Silverberg SC, Major FJ, Blessing JA. Carcinosarcoma (malignant mixed mesodermal tumor) of the uterus. A gynecologic oncology group pathologic study of 203 cases. *Int J Gynecol Pathol* 1990; **9**: 1–19.

2 Davis PC, Franklin EW. Cancer of the vagina. *South Med J* 1975; **68**: 1239.

3 George E, Manivel JC, Dehner LP, Wick MR. Malignant mixed mullerian tumors. An immunohistochemical study of 47 cases, with hitogenetic considerations and clinical correlation. *Hum Pathol* 1991; **22**: 215–23.

4 Neesham D, Kerdemelidis P, Scurry J. Primary malignant mixed mullerian tumor of the vagina. *Gynecol Oncol* 1998; **70**: 303–7.

5 Peters WA, Kumar NB, Anderses WA, Morley GW. Primary sarcoma of the adult vagina: a clinicopathologic study. *Obstet Gynecol* 1985; **65**: 699–704.

6 Rutledge F. Cancer of the vagina. *Am J Obstet Gynecol* 1967; **97**: 635–49.

7 Wada H, Enomoto T, Fujita M *et al.* Molecular evidence that most but not all carcinosarcomas of the uterus are combination tumors. *Cancer Res* 1997; **57**: 5379–85.

8 Fujii H, Yoshida M, Gong ZX *et al.* Frequent genetic heterogeneity in the clonal evolution of gynecological carcinosarcoma and its influence on phenotypic diversity. *Cancer Res* 2000; **60**: 114–20.

9 Sreenan JJ, Hart WR. Carcinosarcomas of the female genital tract. A pathologic study of 29 metastatic tumor: Further evidence for the dominant role of the epithelial component and the conversion theory of histogenesis. *Am J Surg Pathol* 1995; **19**: 666–74.

10 Peters WA, Kumar NB, Fleming WP. Prognostic features of sarcomas and mixed tumors of the endometrium. *Obstet Gynecol* 1984; **63**: 550–56.

11 Colombi RP. Sarcomatoid carcinomas of the female genital tract (malignant mixed mullerian tumors). *Semin Diagn Pathol* 1993; **10**: 169–75.

Pre-B Cell Antigen Receptor-Mediated Signal Inhibits CD24-Induced Apoptosis in Human Pre-B Cells[1]

Tomoko Taguchi,*† Nobutaka Kiyokawa,[2]* Kenichi Mimori,* Toyo Suzuki,* Takaomi Sekino,* Hideki Nakajima,* Masahiro Saito,* Yohko U. Katagiri,* Nobutake Matsuo,‡ Yoshinobu Matsuo,§ Hajime Karasuyama,¶ and Junichiro Fujimoto*

We previously reported that the cross-linking of cluster of differentiation (CD)24 induces apoptosis in Burkitt's lymphoma cells and that this phenomenon can be enhanced by a B cell Ag receptor (BCR)-mediated signal. In this study, we extend our previous observation and report that CD24 also mediated apoptosis in human precursor-B acute lymphoblastic leukemia cell lines in the pro-B and pre-B stages accompanying activation of multiple caspases. Interestingly, simultaneous cross-linking of pre-BCR clearly inhibited CD24-mediated apoptosis in pre-B cells. We also observed that mitogen-activated protein kinases (MAPKs) were involved in the regulation of this apoptotic process. Pre-BCR cross-linking induced prompt and strong activation of extracellular signal-regulated kinase 1, whereas CD24 cross-linking induced the sustained activation of p38 MAPK, following weak extracellular signal-regulated kinase 1 activation. SC68376, a specific inhibitor of p38 MAPK, inhibited apoptosis induction by CD24 cross-linking, whereas anisomycin, an activator of p38 MAPK, enhanced the apoptosis. In addition, PD98059, a specific inhibitor of MEK-1, enhanced apoptosis induction by CD24 cross-linking and reduced the antiapoptotic effects of pre-BCR cross-linking. Collectively, whether pre-B cells survive or die may be determined by the magnitude of MAPK activation, which is regulated by cell surface molecules. Our findings should be important to understanding the role of CD24-mediated cell signaling in early B cell development. *The Journal of Immunology,* **2003, 170: 252–260.**

B cell development is a dramatic process that generates clones that produce Ig having greater affinity for exogenous Ags. In the process, B cells proceed through multiple developmental stages that determine whether they will survive or die, changing their phenotype in a developmental-stage-specific manner (1, 2). In mature B cells, signals transduced through the B cell Ag receptor (BCR),[3] which consists of the μ H chain, conventional κ or λ L chain, Igα, and Igβ, play an essential role in B cell activation and terminal differentiation. In contrast to mature B cells, B cell precursors do not possess the complete form of BCR, but already have alternate Ag receptor complexes. For example, pre-B cells that have successfully accomplished rearrangement of H chain genes start to express a premature form of the Ag receptor, namely, pre-BCR, consisting of the μ H chain, surrogate L chain (V*pre*B and λ5), and the Igα/Igβ heterodimer (3, 4). A number of works have shown the vital importance of pre-BCR as a mediator of pre-B cell differentiation signals (5, 6).

In addition to the Ag receptors, a number of B cell differentiation Ags have been found to mediate signal transduction that leads to proliferation and differentiation upon binding with their specific ligands. Investigation of the stimuli mediated by these surface molecules should therefore provide an approach to understanding the molecular basis of B cell development. Cluster of differentiation (CD)24, also referred to as heat-stable Ag (HSA) in mice, is a B cell differentiation Ag (7). During B cell ontogeny, CD24 is already expressed in very early stage B cell precursors (8), remains expressed on mature resting B cells, and begins to disappear when B cells are activated and induced to further maturation (7, 9–12). This differentiation-dependent expression pattern has implied a role for CD24 in B cell development, and indeed, several lines of evidence suggest functional involvement of CD24 in B cell development. First, CD24 is known to mediate signal transduction, including phosphorylation of intracellular proteins and intracellular calcium mobilization (13–15). In addition, cross-linking of CD24 induces apoptosis in mouse B cell precursors (16, 17). These findings suggest that CD24 is a signal-transducing molecule that acts as a potent negative regulator of B cell development.

In correlation with these findings, we recently reported that CD24 also mediates apoptosis in human Burkitt's lymphoma (BL) cells, which are thought to be related to germinal-center B cells (18). In the findings, we observed a synergism between the cross-linking of CD24 and that of BCR in the effect on apoptosis induction in BL cells, suggesting an interaction between CD24-mediated signaling and that of BCR (18). Because pre-BCR and BCR are structurally related, it is reasonable to expect that CD24 is also

*Department of Developmental Biology, National Research Institute for Child Health and Development, Tokyo, Japan; †Department of Pediatrics, School of Medicine, Keio University, Tokyo, Japan; ‡National Center for Child Health and Development, Tokyo, Japan; §Fujisaki Cell Center, Hayashibara Biochemical Labs Inc., Okayama, Japan; and ¶Department of Immune Regulation, Graduate School, Tokyo Medical and Dental University, Tokyo, Japan

Received for publication December 6, 2001. Accepted for publication October 29, 2002.

The costs of publication of this article were defrayed in part by the payment of page charges. This article must therefore be hereby marked *advertisement* in accordance with 18 U.S.C. Section 1734 solely to indicate this fact.

[1] This work was supported in part by a Grant for Pediatric Research (12C-01) from the Ministry of Health and Welfare of Japan. This work was also supported by a grant from the Japan Health Sciences Foundation for Research on Health Sciences Focusing on Drug Innovation. Additional support was provided by the Program of the Research and Development Promotion Division, Science and Technology Promotion Bureau, Science and Technology Agency for Organized Research Combination System.

[2] Address correspondence and reprint requests to Dr. Nobutaka Kiyokawa, Department of Developmental Biology, National Research Institute for Child Health and Development, 3-35-31, Taishido, Setagaya-ku, Tokyo 154-8567, Japan. E-mail address: nkiyokawa@nch.go.jp

[3] Abbreviations used in this paper: BCR, B cell Ag receptor; BL, Burkitt's lymphoma; CD, cluster of differentiation; HSA, heat-stable Ag; ALL, acute lymphoblastic leukemia; BM, bone marrow; MAPK, mitogen-activated protein kinase; ERK1, extracellular signal-regulated kinase 1; ICAD, an inhibitor of caspase-activated DNase; PARP, poly(ADP-ribose) polymerase; SAPK, stress-activated protein kinase; z-VAD-fmk, z-Val-Ala-Asp-fmk.

0022-1767/03/$02.00

closely correlated with the pre-BCR-mediated signaling system in pre-B cells, although the details are unknown.

To clarify the function of CD24 in early B cell development, we analyzed the effect of cross-linking the molecule in human precursor-B acute lymphoblastic leukemia (ALL) cell lines derived from B cell precursors in bone marrow (BM). Our findings show that cross-linking of CD24 induces apoptosis in two distinct classes of precursor-B ALL cells, namely, pre-B and pro-B ALL cells. They also indicate that the cell signaling that affects mitogen-activated protein kinases (MAPKs) is involved in this apoptotic process. Interestingly, unlike the BCR expressed in BL cells, we further observed that a pre-BCR-mediated signal can inhibit CD24-induced apoptosis in pre-B ALL cells.

Materials and Methods

Cells and reagents

Pre-B ALL-derived cell lines, including HPB-NULL, NALM-6, NALM-17 (19), and P30/OHK (20); Pro-B ALL-derived cell lines, including NALM-16, NALM-20, NALM-27 (19), LC4-1 (21), and KM-3 (22); and $CD24^+$ BL-derived cell line BALM-24 were used. Cells were cultured in RPMI 1640 supplemented with 10% FCS at 37°C in a humidified 5% CO_2 atmosphere.

The mouse mAbs used were: anti-CD24 (L30) (9); anti-μ (DA4.4) from American Type Culture Collection (Manassas, VA); antiextracellular signal-regulated kinase 1 (ERK1) and anti-caspase-2, -3, and -7 from BD Transduction Laboratories (Lexington, KY); anti-caspase-8 and anti-inhibitor of caspase-activated DNase (ICAD) from Medical & Biological Laboratories (Nagoya, Japan); and anti-poly(ADP-ribose) polymerase (PARP) from Biomol (Plymouth Meeting, PA). The polyclonal Abs used were: anti-p38 MAPK and anti-stress-activated protein kinase (SAPK) from New England Biolabs (Beverly, MA); anti-actin from Santa Cruz Biotechnology (Santa Cruz, CA); anti-GST from Boehringer Mannheim (Indianapolis, IN). All anti-phospho-specific Abs and all anticleaved caspase Abs were purchased from New England Biolabs. Secondary Abs, including fluorescein-conjugated and enzyme-conjugated Abs, were purchased from Jackson ImmunoResearch Laboratories (West Grove, PA). Biotinylation and FITC-conjugation of mAb was performed as described previously (10). To cross-link CD24, the combinations of either purified L30 (5 μg/ml) and secondary anti-mouse Ig Ab (10 μg/ml) or biotinylated L30 (10 μg/ml) and avidin (20 μg/ml) (Sigma-Aldrich, St. Louis, MO) were used. To cross-link pre-BCR, purified DA4.4 (5 μg/ml) was used. In these cases, Abs were dialyzed in medium before being introduced to culture to remove additives. A peptide inhibitor for a broad spectrum of caspases, z-Val-Ala-Asp-fmk (z-VAD-fmk), was obtained from Bachem (Torrence, CA). The MEK-1 inhibitors PD98059 and U0126 were purchased from Calbiochem (La Jolla, CA) and New England Biolabs, respectively. The p38 MAPK inhibitor SC68376 and p38 MAPK activator anisomycin were purchased from Calbiochem. The GST-ATF-2 and GST-ELK-1 fusion proteins were purchased from New England Biolabs. All chemical reagents were obtained from Wako Pure Chemical (Osaka, Japan), unless otherwise indicated.

Immunofluorescence study and detection of apoptosis

Cells were stained with FITC-labeled mAbs and analyzed by flow cytometry (EPICS-XL; Beckman Coulter, Fullerton, CA) as described previously (10). To quantify the incidence of apoptotic cells, cells were stained with FITC-labeled annexin V using a MEBCYTO-Apoptosis kit (Medical & Biological Laboratories) and then analyzed by flow cytometry according to the manufacturer's protocol. Experiments were performed in triplicate, and the means ± SDs of the cells that bound annexin V are shown. Caspase-3 activity was assessed with a PhiPhiLux G1D2 kit (Medical & Biological Laboratories) and analyzed by flow cytometry according to the manufacturer's protocol.

Immunoblotting and in vitro kinase assay

Cell lysates were prepared by dissolving cells in lysis buffer, and the protein concentration of each cell lysate was determined as described previously (23). A 50-μg quantity of each whole cell lysate was electrophoretically separated on an SDS-polyacrylamide gel and transferred to a nitrocellulose membrane by a semidry transblot system (Bio-Rad, Hercules, CA). Immunoblotting was performed as described previously (23).

To test p38 MAPK activity, 500 μg of cell lysate was incubated with 2 μg of anti-p38 MAPK Ab in the presence of 30 μl of 50% protein G-agarose (Boehringer Mannheim) for 1 h. After intensive washing, the immunoprecipitates were mixed with 2 μg of GST-ATF-2 fusion protein as exogenous substrate. Transphosphorylation activity of p38 MAPK was determined by two types of assay. First, the mixture was incubated for 20 min at room temperature in 30 μl of kinase assay buffer (50 mM Tris-HCl, pH 7.5; 10 mM $MgCl_2$; 1 mM DTT; 1 mM EGTA; 100 μM ATP) with 10 μCi of [γ-^{32}P]ATP (specific activity >3000 Ci/mM; NEN, Boston, MA). Reactions were stopped by adding 6 μl of 6× SDS-sample loading buffer (23). After separation on a 10% SDS-PAGE gel, phosphorylated proteins were visualized with autoradiography as described previously (23). Alternatively, the kinase reaction was performed as described above but without the use of [γ-^{32}P]ATP. Subsequent incorporation of nonisotopic phosphates into substrate was determined by immunoblotting using anti-phospho-ATF-2 Ab. The ERK1 kinase activity was examined similarly by using GST-ELK-1 fusion protein as substrate.

Results

Cross-linking of CD24 induces apoptosis in pre-B and pro-B ALL cell lines

First, we tested whether cross-linking of CD24 induces apoptosis in precursor-B ALL cells, including pre-B and pro-B ALL cells, expressing CD24 (Fig. 1*A*), as is the case with murine pre-B cells (17). When pre-B HPB-NULL cells were exposed to anti-CD24 mAb in the presence of secondary rabbit polyclonal anti-mouse Ig Ab, a significant number of annexin-V-bound cells appeared in a time-dependent manner (Fig. 1*B*). We also examined combinations of biotinylated anti-CD24 mAb and avidin, and obtained identical results (Fig. 1*C*). These phenomena were specific to CD24 because other mAbs, such as anti-CD22 and anti-CD72, both of which bind to HPB-NULL cells, did not induce apoptosis (data not shown). We similarly examined other pre-B and pro-B ALL cell lines and obtained essentially the same results, but pro-B NALM-27 and NALM-16 cells showed much less sensitivity to induction of CD24-mediated apoptosis than was observed in the other cells (Fig. 1, *D* and *E*). These findings suggest that induction of apoptosis upon CD24 cross-linking is a feature common to pre-B and pro-B ALL cell lines expressing CD24, but that the magnitude of cell death is variable. By contrast, when KM-3 pro-B cells, which do not express CD24, were similarly examined (Fig. 1*F*), treatment with a combination of anti-CD24 mAb and rabbit anti-mouse Ig Ab failed to induce apoptosis (Fig. 1*F*), indicating that CD24 cross-linking specifically induces apoptosis in CD24-expressing cells, and that this is not due to the nonspecific binding of either mouse Ig or secondary rabbit polyclonal anti-mouse Ig Ab.

Activation of caspases in the course of CD24-mediated apoptosis

A number of studies have indicated that caspases are essential as effector molecules in the apoptotic process in most cases (24). Therefore, we investigated whether caspases are activated during the apoptotic process induced by cross-linking CD24 in HPB-NULL cells. As shown in Fig. 2, *A* and *B*, immunoblot analysis revealed cleavage of caspases, including caspases-8, -3, -2, and -7, in HPB-NULL cells after CD24 cross-linking in parallel with the appearance of annexin-V-bound cells (Fig. 1*C*), indicating activation of the caspases. Cleavage of PARP and ICAD, which are known to be substrates of caspases, was also consistently observed (Fig. 2, *A* and *B*). We also tested the activity of caspase-3 in individual cells by using PhiPhiLux G1D2. As shown in Fig. 2*C*, a significant increase in fluorescence activity was observed after CD24 cross-linking. These findings indicate that multiple caspases are activated during the course of CD24-mediated apoptosis in pre-B ALL cells, and evidence that this apoptotic process is inhibited by z-VAD-fmk (Fig. 2*D*), a specific peptide inhibitor of caspases, further supports this idea.

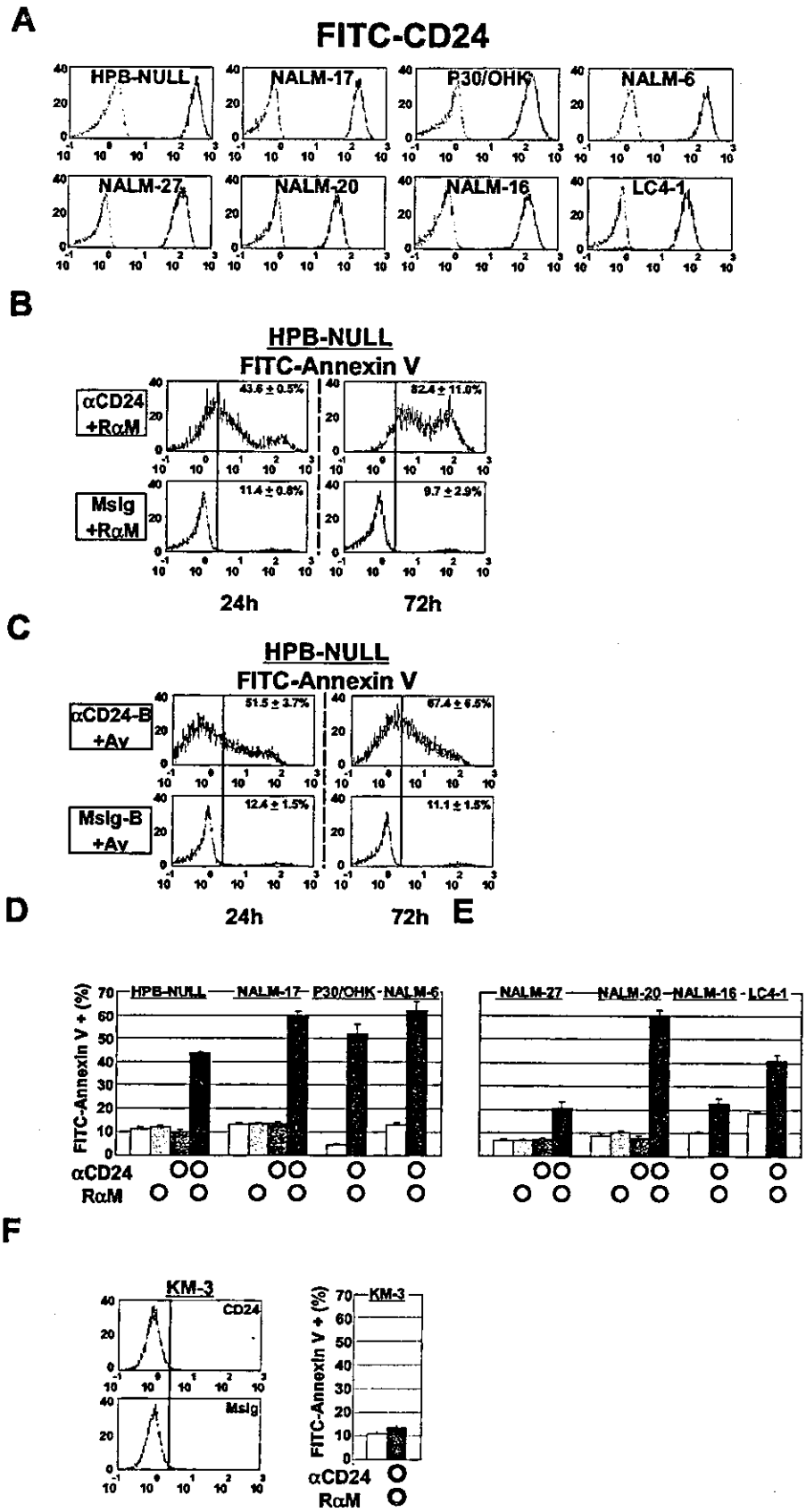

FIGURE 1. Induction of apoptosis mediated by cross-linking of CD24 in pre-B and pro-B ALL cells. *A*, Expression of CD24 on pre-B and pro-B ALL cell lines was examined by flow cytometry. The histograms obtained (dark lines) have been superimposed on those of the negative control (cells stained with isotype-matched control mouse Ig, light lines) and displayed. *x*-axis, fluorescence intensity; *y*-axis, relative cell number. *B*, Pre-B ALL HPB-NULL cells (2.5×10^5 cells in 500 μl of medium) were exposed to either anti-CD24 mAb L30 (αCD24, *upper panels*) or isotype-matched control mouse Ig (MsIg, *lower panels*) in the presence of secondary rabbit anti-mouse Ig Ab (RαM) for the periods indicated. At the end of the culture period, HPB-NULL cells were stained with FITC-conjugated annexin V and analyzed by flow cytometry. *C*, HPB-NULL cells were treated with either biotinylated anti-CD24 mAb L30 (αCD24-B, *upper panels*) or biotinylated isotype-matched control mouse Ig (MsIg-B, *lower panels*) in the presence of avidin (Av) and examined as in *B*. *D*, The pre-B ALL cell lines indicated were treated as in *B* for 24 h, and the annexin-V-bound cells were detected in a similar manner. *E*, The pro-B ALL cell lines indicated were examined as in *D*. *F*, CD24$^-$ pro-B ALL KM-3 cells were examined as in *A* and *D*.

Activation of MAPK mediated by cross-linking of CD24

In other cell types, it has been reported that cross-linking of CD24 results in intracellular signaling events such as the activation of protein kinases (13, 18, 25–28). It has also been shown that MAPKs are involved in determining whether a cell survives or undergoes apoptosis in several cases (29, 30). Thus, we attempted to examine the changes in MAPK activity after CD24 cross-linking in pre-B cells.

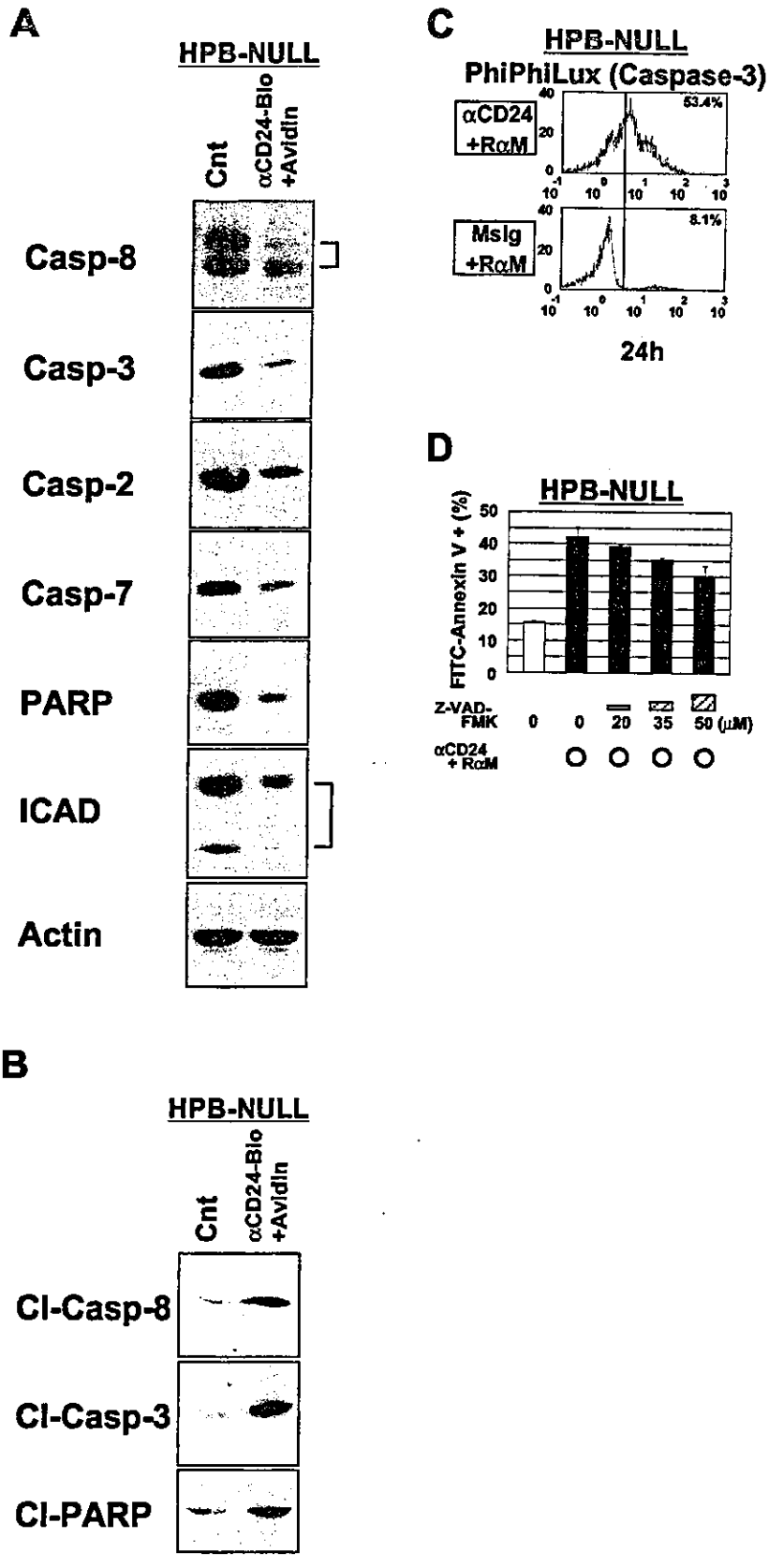

FIGURE 2. Activation of caspases in the course of CD24-mediated apoptosis in HPB-NULL cells. *A*, In parallel with the experiment presented in Fig. 1*C*, cell lysates were prepared. The proforms of each caspase and caspase substrate were detected by immunoblotting with Abs as indicated. Cnt, treated with biotinylated isotype-matched control mouse Ig and avidin; αCD24-Bio, biotinylated anti-CD24 mAb; Casp-, caspase. *B*, In parallel with *A*, the cleaved forms of each caspase and PARP were detected with Abs as indicated. Cl-, cleaved. *C*, Caspase-3 activity in the same sample preparation as in Fig. 1*B* was examined using PhiPhiLux G1D2. *D*, After 1-h preincubation with different concentrations of z-VAD-fmk, a peptide inhibitor of caspases, HPB-NULL cells were exposed to a combination of anti-CD24 mAb L30 (αCD24) and secondary rabbit anti-mouse Ig Ab (RαM) as in Fig. 1*D*. The subsequent incidence of apoptotic cells was determined.

When the total cell lysates prepared from CD24-cross-linked HPB-NULL cells were examined by immunoblotting with Abs that specifically recognize phosphorylated MAPKs, clear increases in the phosphorylations of p38 MAPK and ERK1 were detected (Fig. 3*A*), while the protein amounts of these kinases did not change during the course of stimulation (Fig. 3*A*). In vitro kinase assay revealed that the phosphorylations of these kinases were indeed accompanied by an elevation of the kinase activity (Fig. 3, *B* and *C*). These findings suggest that CD24 cross-linking activates both kinases. Interestingly, the activation of these kinases occurred

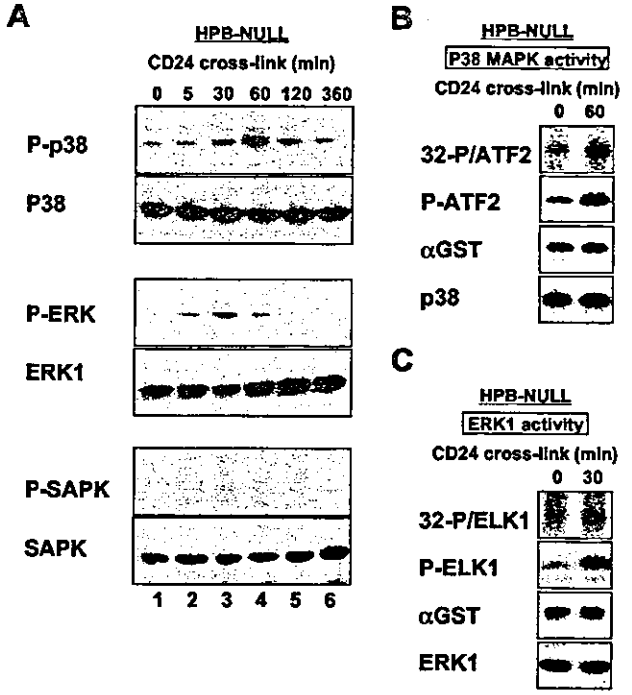

FIGURE 3. Activation of MAPKs in HPB-NULL cells mediated by CD24 cross-linking. *A*, Protein lysates were prepared from HPB-NULL cells exposed to (*lanes 2–6*) or not exposed to (*lane 1*) the combination of biotinylated anti-CD24 mAb and avidin (CD24 cross-link) for the periods indicated. Each cell lysate was electrophoretically separated on 10% SDS-PAGE gels and immunoblotted with specific Abs against the MAPKs indicated. P-p38, phosphorylated p38 MAPK; P-ERK, phosphorylated ERK; P-SAPK, phosphorylated SAPK. *B*, The immunoprecipitates with anti-p38 MAPK Ab were prepared in triplicate from cell lysates described in *A*. In vitro kinase assay was performed using GST-ATF-2 as a substrate. In addition to conventional kinase assay using [γ-^{32}P]ATP (32-P/ATF2), transphosphorylation activity of p38 MAPK was also assessed by immunoblotting using a combination of nonisotopic ATP and specific Ab against phosphorylated ATF-2 (P-ATF2). After stripping the Abs, the membrane was reproved with anti-GST Ab to test the protein amounts of the substrate in each reaction (αGST). The p38 MAPK proteins in each immunoprecipitate were detected by immunoblotting (p38). *C*, Transphosphorylation activity of ERK1 was also assessed by in vitro kinase assay as in *B* using GST-ELK-1 as a substrate.

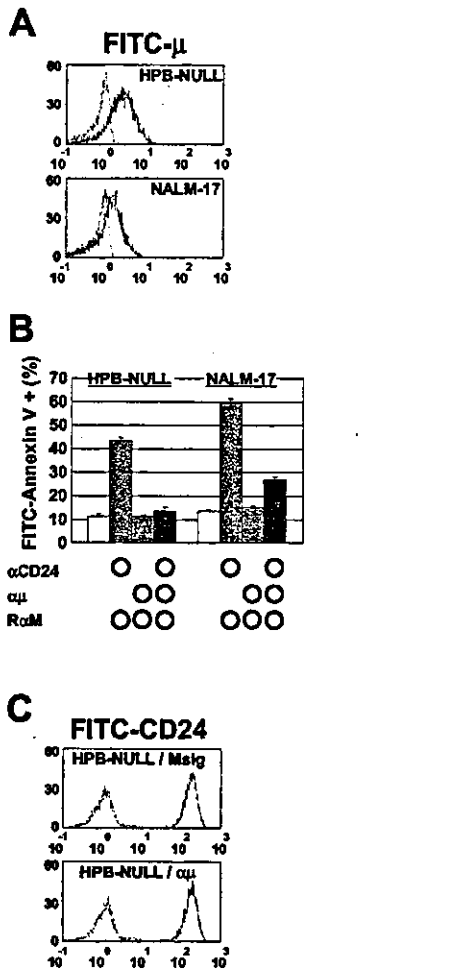

FIGURE 4. Effect of simultaneous cross-linking of pre-BCR with CD24 on the induction of apoptosis in pre-B ALL cells. *A*, Expression of the μ H chain on pre-B ALL cell lines was examined as in Fig. 1*A*. *B*, Pre-B ALL cell lines HPB-NULL and NALM-17 were exposed to and not exposed to anti-CD24 mAb (αCD24) and anti-μ H chain mAb ($\alpha\mu$) in the presence or absence of secondary rabbit anti-mouse Ig Ab (RαM) as indicated. After 24-h cultivation, cells were examined as in Fig. 1*D*. *C*, HPB-NULL cells preincubated with an excess amount (40 μg/ml) of either $\alpha\mu$ or isotype-matched control mouse Ig (MsIg) were stained with FITC-conjugated αCD24 and analyzed by flow cytometry as in Fig. 1*A*.

in a nonsynchronous manner. As shown in Fig. 3*A*, the phosphorylation of ERK1 peaked at 30 min after CD24 cross-linking and then decreased to the resting level at 120 min. By contrast, the peak activation of p38 MAPK was observed at 60 min after CD24 cross-linking, and it remained activated at 120 min (Fig. 3*A*). Activation of SAPK (Fig. 3*A*) and ERK5 (data not shown) was not detected after CD24 cross-linking.

Simultaneous cross-linking of pre-BCR inhibits CD24-mediated apoptosis in HPB-NULL cells

As previously reported (19), and shown in Fig. 4*A*, HPB-NULL cells express a considerable amount of pre-BCR on their cell surface. Because pre-BCR is thought to mediate the proliferation and differentiation signals in pre-B cells (31), we tested the effect of simultaneous cross-linking of pre-BCR on the apoptosis induction mediated by CD24 and found that the CD24-mediated apoptosis was significantly inhibited in the presence of anti-μ mAb (Fig. 4*B*). We also tested other pre-B ALL lines (Fig. 4, *A* and *B* and data not shown) and observed mostly identical results. As shown in Fig. 4*C*, when HPB-NULL cells previously exposed to an excess of anti-μ mAb were stained with FITC-conjugated anti-CD24 mAb, no significant reduction in consequent fluorescein intensity was observed. Therefore, the inhibition of CD24-mediated apoptosis by anti-μ mAb is not merely the result of inhibition of the binding of anti-CD24 mAb to the cells.

To address the mechanism of pre-BCR-mediated inhibition of CD24-induced apoptosis, we examined the intracellular signaling events following the cross-linking of pre-BCR. As shown in Fig. 5*A*, immunoblotting analysis revealed prompt and strong activation of ERK1 after pre-BCR cross-linking. The phosphorylation of ERK1 increased to its maximal level at 5 min after stimulation and decreased quickly thereafter. By contrast, p38 MAPK and SAPK presented very weak and transient phosphorylation after pre-BCR cross-linking (Fig. 5*A*).

Involvement of MAPKs in apoptosis induction induced by CD24 cross-linking and pre-BCR-mediated inhibition of the apoptosis

Because it was recently reported that MAPKs have opposite effects on the induction of apoptosis and that ERK1 induces cell survival signals in a variety of cell types, whereas p38 MAPK and SAPK mediate apoptotic signals (29, 30), we examined whether change

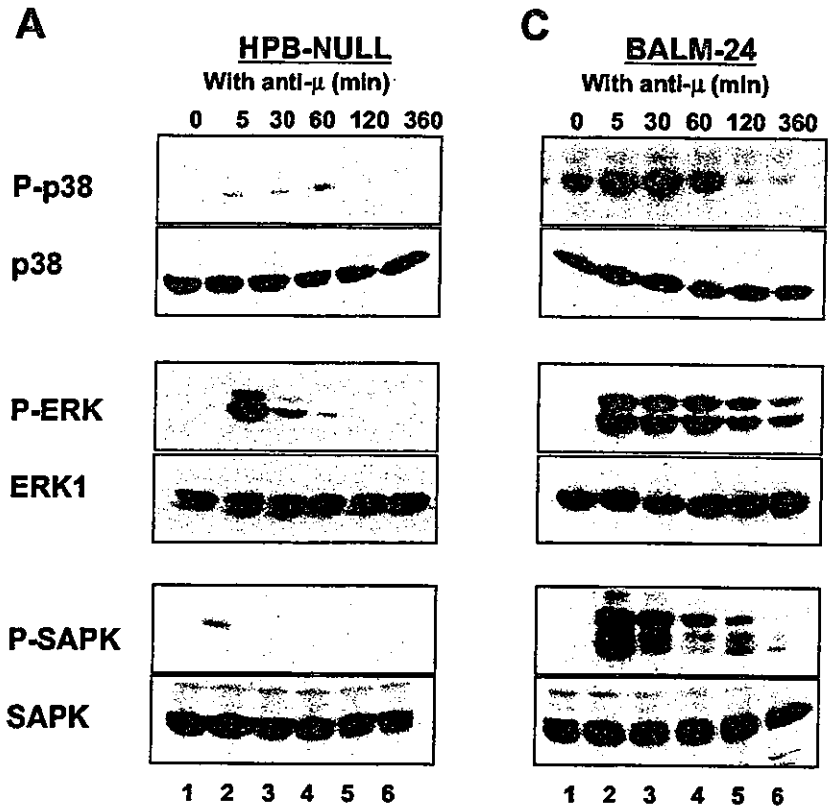

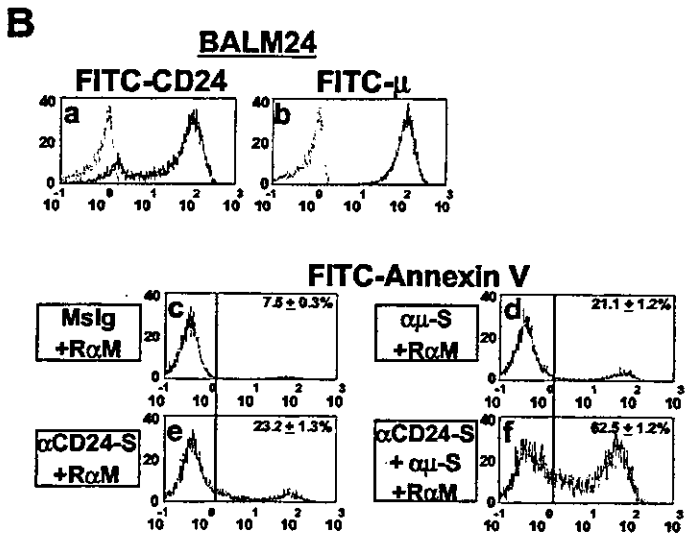

FIGURE 5. Activation of MAPKs mediated by pre-BCR in pre-B cells and by BCR in BL cells. *A*, Protein lysates were prepared from pre-B HPB-NULL cells exposed (*lanes 2–6*) or unexposed (*lane 1*) to anti-μ H chain mAb for the periods indicated. Each cell lysate was analyzed by immunoblotting with the Abs indicated. P-p38, phosphorylated p38 MAPK; P-ERK, phosphorylated ERK; P-SAPK, phosphorylated SAPK. *B*, Expression of CD24 (*a*) and the μ H chain (*b*) on BL BALM-24 cells was examined by flow cytometry as in Fig. 1*A*. BALM-24 cells were exposed to and not exposed to suboptimal doses of anti-CD24 mAb (α CD24-S, 2.5 μg/ml) and anti-μ H chain mAb (α μ-S, 0.1 μg/ml) in the presence of 5 μg/ml of secondary rabbit anti-mouse Ig Ab as indicated (*c–d*). After 24-h cultivation, the subsequent incidence of apoptotic cells was examined as in Fig. 1*B*. *C*, Activation of MAPKs after BCR cross-linking in BALM-24 cells were examined as in *A*.

in p38 MAPK activity has any effect on CD24-mediated apoptosis. As shown in Fig. 6*A*, pretreatment with SC68376, a selective p38 MAPK inhibitor (32, 33), inhibited CD24-mediated apoptosis in a dose-dependent manner. In parallel, immunoblotting analysis revealed that SC68376 indeed inhibited the activation of p38 MAPK induced by CD24 cross-linking (Fig. 6*B*). By contrast, pretreatment with anisomycin, a strong activator of p38 MAPK (34, 35), activated p38 MAPK (Fig. 6*D*) and enhanced CD24-mediated apoptosis in a dose-dependent manner (Fig. 6*C*).

We next examined whether inhibition of ERK1 activity has any effect on CD24-mediated apoptosis. As shown in Fig. 6*E*, pretreatment with PD98059, an MEK-1 inhibitor (36, 37), clearly enhanced CD24-mediated apoptosis in a dose-dependent manner. In parallel, immunoblotting analysis revealed that PD98059 indeed inhibited the activation of ERK1 induced by CD24 cross-linking (Fig. 6*F*). It is noteworthy that pretreatment with PD98059 also markedly inhibited the activation of ERK1 induced by pre-BCR cross-linking (Fig. 6*G*), and that simultaneous cross-linking of pre-BCR was no longer sufficient to effectively inhibit CD24-mediated apoptosis (Fig. 6*E*). Essentially identical results were obtained when another inhibitor of MEK-1/2, U0126, was used (data not shown).

Activation of MAPKs is mediated by the cross-linking of BCR in BL cells

We previously reported that the cross-linking of CD24 induces apoptosis in BL cells (18). In this phenomenon, however, a synergism

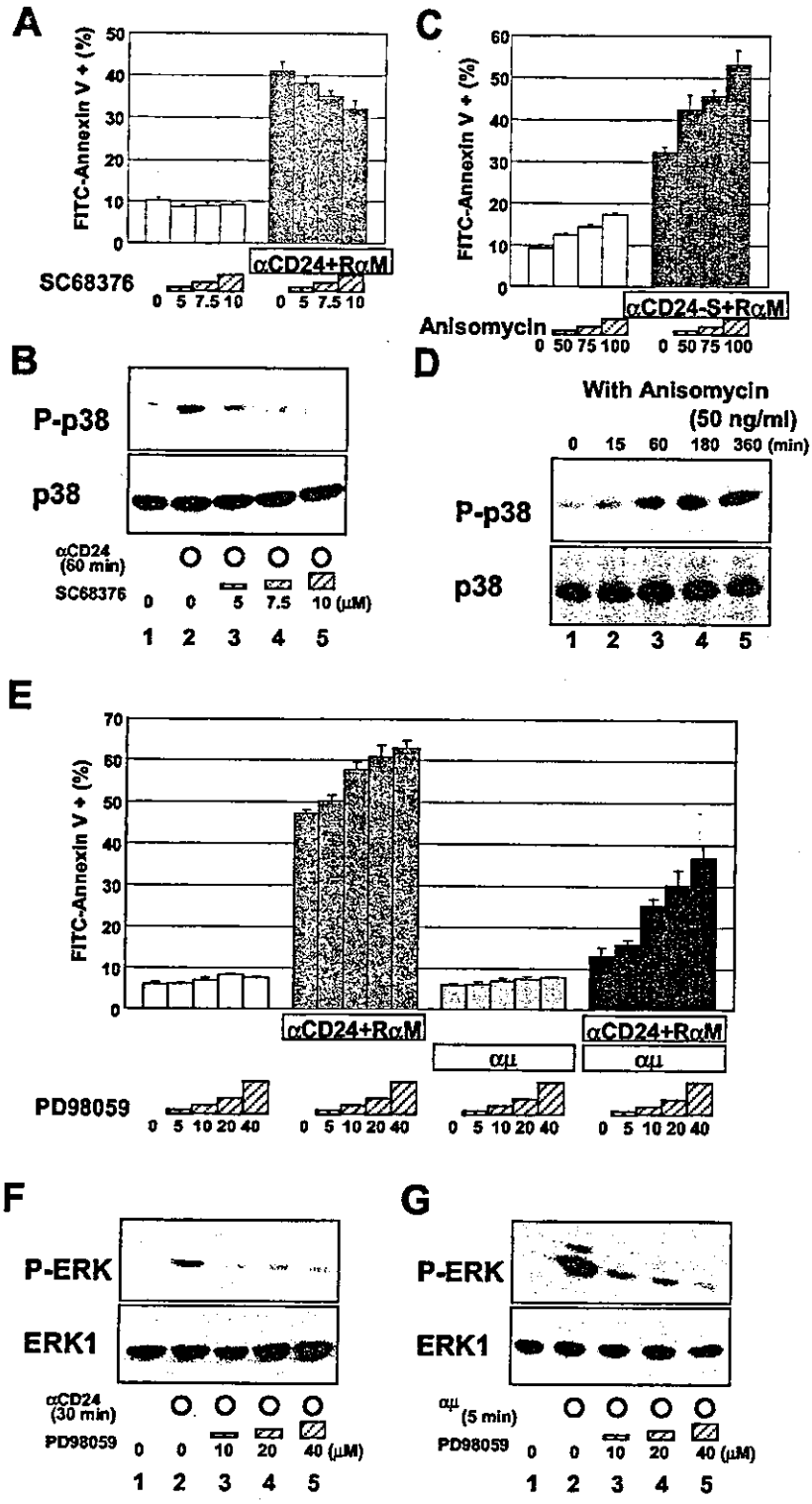

FIGURE 6. Effect of kinase inhibitors and activator on CD24-mediated apoptosis in pre-B ALL cells. *A*, HPB-NULL cells were preincubated with p38 MAPK inhibitor SC68376 for 1 h. After being exposed to anti-CD24 mAb in the presence of secondary rabbit anti-mouse Ig Ab (RαM) for 24 h, annexin-V-bound cells were detected as in Fig. 1*D*. *B*, HPB-NULL cells were preincubated (*lanes 3–5*) or not incubated (*lanes 1* and *2*) with the indicated amount of SC68376 for 1 h. After being exposed or unexposed to the combinations of Abs indicated for 60 min, cell lysates were prepared and immunoblotting analysis was performed as in Fig. 3. P-p38, phosphorylated p38 MAPK. *C*, HPB-NULL cells were preincubated with indicated concentrations of p38 MAPK activator anysomycin for 1 h. After being exposed to the combination of suboptimal doses of anti-CD24 mAb (αCD24-S, 3.5 μg/ml) and secondary RαM for 24 h, annexin-V-bound cells were detected as in Fig. 1*D*. *D*, Protein lysates were prepared from HPB-NULL cells treated with anysomycin (50 ng/ml) for the periods indicated, and immunoblotting analysis was performed as in Fig. 3. *E*, HPB-NULL cells were preincubated with MEK-1 inhibitor PD98059 for 1 h. After being exposed to the combinations of Abs indicated for 24 h, annexin-V-bound cells were detected as in Fig. 1*D*. *F*, HPB-NULL cells were preincubated (*lanes 3–5*) or not incubated (*lanes 1* and *2*) with the indicated amount of PD98059 for 1 h. After being exposed or unexposed to anti-CD24 mAb in the presence of RαM (αCD24) for 30 min, cell lysates were prepared and immunoblotting analysis was performed as in Fig. 3. P-ERK, phosphorylated ERK. *G*, HPB-NULL cells were preincubated with PD98059 for 1 h as in *D*. After being exposed or unexposed to anti-μ H chain mAb for 5 min, cell lysates were prepared and immunoblotting analysis was performed as in Fig. 3.

was observed between the cross-linking of CD24 and that of BCR in their effect on apoptosis induction. As shown in Fig. 5*B*, both anti-CD24 mAb (*e*) and anti-μ H chain mAb (*d*) failed to induce significant apoptosis in $CD24^+$ BL cell line BALM-24 at suboptimal doses (1.25 and 0.1 μg/ml, respectively). When suboptimal doses of both anti-CD24 mAb and anti-μ H chain mAb were mixed, however, a significant level of apoptosis was induced in BALM-24 cells (Fig. 5*Bf*). To address the difference between the regulatory mechanism of CD24-mediated apoptosis by BCR-mediated signals in BL cells and that by pre-BCR in pre-B ALL cells, we examined the changes in MAPK activity after BCR cross-linking in BL cells. Like the example of pre-BCR cross-linking in pre-B ALL cells (Fig. 5*A*), an immunoblotting analysis revealed the prompt and strong phosphorylation of ERK1 in BALM-24 BL cells following BCR cross-linking (Fig. 5*B*). Simultaneously, the distinct phosphorylation of both p38 MAPK and SAPK was observed in BALM-24 cells after BCR cross-linking (Fig. 5*B*). This phenomenon was quite unlike the case of pre-BCR cross-linking in pre-B ALL cells, in which both kinases were phosphorylated only faintly (Fig. 5*A*).

Discussion

Our findings clearly indicate that the cross-linking of CD24 induces apoptosis in human precursor-B ALL cells, including pro-B and pre-B ALL cells. Consistent with our observations, Chappel et al. demonstrated that the cross-linking of HSA, a mouse homolog of CD24, induces apoptosis in murine B cell precursors in BM (17) and concluded that HSA acts as a negative regulator of B cell precursors in a physiological context. Ligation of HSA may assist in the elimination of undesirable B cell precursors, such as cells with aberrant or nonproductive H chain and L chain gene rearrangements, or cells that display self-specificity (17). Our research allows their hypothesis to be expanded to include a potential role for CD24 as a negative regulator of B cell precursors in humans.

In addition to B cell precursors, CD24 was found to affect other B-lineage cells as a negative regulator, but its effect depends on the stage of B cell differentiation. For example, Chappel et al. observed an inhibitory, but not apoptotic, effect of HSA cross-linking on proliferation of murine mature resting B cells (17), while we recently reported that CD24 cross-linking induces apoptosis in BL cells, which are thought to be related to germinal center B cells in lymphoid follicles (18). Among B cell precursors in mice, IL-7-responsive clonogenic progenitors, consisting mainly of pre-B cells, have been found to display the greatest sensitivity to HSA-mediated apoptosis despite no significant difference in cell surface HSA expression compared with other B-lineage cell populations in BM (16, 17). Consistent with these observations, we found that all pre-B ALL lines tested exhibited significant induction of apoptosis after CD24 cross-linking, whereas some pro-B ALL lines are less sensitive to CD24-mediated apoptosis. All of these findings suggest differential effects of CD24 cross-linking at different stages of B cell development.

We observed activation of multiple caspases in the process of CD24-mediated apoptosis in precursor-B ALL cells. The caspases are thought to be essential as effector molecules in the many cases of apoptotic process (24). Caspases exist in the cells as inactive proenzymes and become activated upon cleavage and the subsequent heterotetramerization of the cleaved subunits. Caspases themselves have also been shown to form a regulatory cascade that transduces apoptotic signals. Apoptotic stimuli mediated by cell surface molecules induce the activation of upstream caspases, such as caspase-8 and -6, which subsequently cleave downstream caspases, such as caspase-3, -2, and -7 (38). The downstream caspases go on to cleave various cellular substrates, including PARP, fodrin, lamin, and ICAD, all of which are responsible for apoptosis (38). Our findings suggest that CD24 cross-linking initiates just such a caspase cascade. Additional experiments to better define the mechanism by which CD24 initiates this process are now under way.

We noted the activation of MAPKs, including ERK1 and p38 MAPK, but not SAPK, after CD24 cross-linking in pre-B cells. It was recently shown that ERK1 induces cell proliferation and differentiation signals in a variety of cell types, while activation of p38 MAPK and SAPK mediate apoptotic signaling (29, 30). For example, ERK1 signaling leads to the promotion of cell survival in NGF-differentiated PC-12 cells, whereas activation of p38 MAPK and SAPK induces apoptosis (29). Activation of the ERK1 cascade in T cells is sufficient to provide positive selection signals, whereas the p38 MAPK signaling pathway has been found to be critical in inducing negative selection of developing T cells in mouse thymocytes (30). These observations suggest that ERK1 and p38 MAPK may antagonize each other by a direct or indirect mechanism, and that the dynamic balance between these MAPKs may be important in determining whether a cell survives or undergoes apoptosis (29). In view of this evidence, it is reasonable to hypothesize that ERK1 and p38 MAPK are also involved in determining the survival or death of pre-B cells. As shown by this study, CD24 cross-linking induced the activation of ERK1 and p38 MAPK. But the kinetics and magnitude of the activation of these kinases were different, and the activations of p38 MAPK are delayed and/or sustained. Thus, the death signal mediated by p38 MAPK may overcome the survival signal mediated by ERK1 in these cells. The fact that both inhibition of ERK1 activity by MEK-1 inhibitor PD98059 and activation of p38 MAPK activity by anisomycin enhance CD24-mediated apoptosis, while inhibition of p38 MAPK activity by a selective inhibitor such as SC68376 retards apoptosis, appears to support this notion.

We have described how CD24-mediated apoptosis is inhibited by pre-BCR-mediated stimuli in pre-B cells. A series of subsequent analyses of precursor-B cells in normal and mutant mice has revealed the involvement of pre-BCR in several events critical to early B cell development (31, 39–41), including the differentiation of pre-B cells and the selective amplification of μ H chain-producing pre-B cells by driving the cell cycle. Therefore, the regulation of CD24-mediated apoptosis by pre-BCR-mediated signaling may play a role in early B cell development. Although the precise mechanism by which pre-BCR-mediated signals inhibit CD24-mediated apoptosis remains unclear, our data suggest the involvement of MAPK-mediated signaling in this process. As shown by this study, cross-linking of pre-BCR induces prompt and intensive activation of ERK1, which may inhibit the death signaling by CD24, upon simultaneous stimulation of CD24 and pre-BCR. Indeed, inhibition of ERK1 activity by PD98059 reduces the inhibitory effect of pre-BCR-mediated signaling against the CD24-mediated apoptotic process.

It is noteworthy, however, that CD24-mediated stimuli augmented BCR-mediated apoptosis induction in BL cells, as reported previously (18). The correlation between CD24- and Ag-receptor-mediated stimuli may differ according to the stage of B cell development. Thus, BCR-mediated signals in BL cells and pre-BCR-mediated signals in precursor-B ALL cells have the opposite effect on CD24-mediated apoptosis. Because the expression pattern of signaling molecules in B cells varies according to the developmental stage, even though pre-BCR and BCR are structurally related the signaling molecules located downstream from each Ag receptor should be different. The differences between the regulatory mechanisms of CD24-mediated apoptosis by pre-BCR in pre-B cells and that by BCR in BL cells are presently not known. However, we observed that the cross-linking of BCR activates all three MAPKs, including ERK1, p38 MAPK, and SAPK, in BL cells, whereas pre-BCR activates only ERK1 in pre-B cells. Considering the evidence that ERK1 mediates cell survival signaling whereas p38 MAPK and SAPK mediate apoptotic signaling, our findings concerning the different activation patterns of MAPKs by pre-BCR and BCR may explain the opposite effects of these receptors on CD24-mediated apoptosis, at least in part.

In conclusion, our findings suggest that CD24-mediated apoptosis is a model for the cell death of B cell precursors in BM. Although additional studies are clearly necessary, investigation of the mechanism of CD24-mediated apoptosis and its inhibition by pre-BCR-mediated signaling should provide a new approach to understanding the regulation of early B cell development and lead to the establishment of a new therapeutic strategy for precursor-B ALL.

Acknowledgments

We thank M. Sone and S. Yamauchi for their excellent secretarial work.